Endoplasmic reticulum stress differentially inhibits endoplasmic reticulum and inner nuclear membrane protein quality control degradation pathways

Received for publication, July 22, 2019, and in revised form, November 4, 2019 Published, Papers in Press, November 13, 2019, DOI 10.1074/jbc.RA119.010295

Bryce W. Buchanan[‡1], **Adrian B. Mehrtash**[§2], **Courtney L. Broshar**[‡2], **Avery M. Runnebohm**[‡3], **Brian J. Snow**[‡4], **Laura N. Scanameo**[‡], **Mark Hochstrasser**[§¶], and **Eric M. Rubenstein**[‡5]

From the [‡]*Department of Biology, Ball State University, Muncie, Indiana 47306 and the Departments of* [¶]*Molecular Biophysics and Biochemistry and* [§]*Molecular, Cellular, and Developmental Biology, Yale University, New Haven, Connecticut 06520*

Edited by George N. DeMartino

Endoplasmic reticulum (ER) stress occurs when the abundance of unfolded proteins in the ER exceeds the capacity of the folding machinery. Despite the expanding cadre of characterized cellular adaptations to ER stress, knowledge of the effects of ER stress on cellular physiology remains incomplete. We investigated the impact of ER stress on ER and inner nuclear membrane protein quality control mechanisms in *Saccharomyces cerevisiae*. We analyzed the turnover of substrates of four ubiquitin ligases (Doa10, Rkr1/Ltn1, Hrd1, and the Asi complex) and the metalloprotease Ste24 in induced models of ER stress. ER stress did not substantially impact Doa10 or Rkr1 substrates. However, Hrd1-mediated destruction of a protein that aberrantly engages the translocon (*Deg1*-Sec62) and substrates with luminal degradation signals was markedly impaired by ER stress; by contrast, Hrd1-dependent degradation of proteins with intramembrane degrons was largely unperturbed by ER stress. ER stress impaired the degradation of one of two Asi substrates analyzed and caused a translocon-clogging Ste24 substrate to accumulate in a form consistent with persistent translocon occupation. Degradation of *Deg1*-Sec62 in the absence of stress and stabilization during ER stress were independent of four ER stress–sensing pathways. Our results indicate ER stress differentially impacts degradation of protein quality control substrates, including those mediated by the same ubiquitin ligase. These observations suggest the existence of additional regulatory mechanisms dictating substrate selection during ER stress.

Eukaryotic cells possess sensitive mechanisms to detect and respond to a variety of external and intrinsic stresses. One such stress is the increased abundance of misfolded and unfolded proteins in the endoplasmic reticulum (ER).[6] Cells and organisms have evolved a multipronged approach to cope with ER stress.

Much of what has been learned about the cellular response to ER stress was first discovered in *Saccharomyces cerevisiae*. The prototypical branch of the ER stress response is the unfolded protein response (UPR) (1). In budding yeast, accumulation of misfolded proteins in the ER activates the transmembrane protein Ire1 (in mammals, the UPR has expanded to include two additional transmembrane signal transducers, PERK and ATF6). The cytoplasmic portion of Ire1 carries both kinase and RNase domains. Binding to unfolded proteins by the luminal domain triggers multimerization of Ire1, which undergoes trans-autophosphorylation and RNase activation. This, in turn, stimulates Ire1-dependent noncanonical splicing of the mRNA encoding the Hac1 transcription factor (Xbp1 in mammals), allowing Hac1 protein translation. Hac1 activates an expansive gene expression program to restore ER homeostasis.

Genes induced by Hac1 include those encoding ER-localized chaperones (such as Kar2/BiP) to facilitate protein folding and components of the ER-Associated Degradation (ERAD) machinery to promote proteasomal turnover of aberrant polypeptides that cannot be correctly folded (2). At least four ubiquitin ligases (E3s), Doa10, Hrd1, Rkr1 (also called Ltn1), and Ubr1, promote ERAD of aberrant ER proteins in yeast cells (3–9). Doa10 and Hrd1 are transmembrane proteins with cytosolic catalytic domains (10, 11), whereas Rkr1 and Ubr1 are soluble cytosolic enzymes (12, 13). Doa10 also resides in the

This work was supported by Ball State University ASPiRE Research Awards (to B. W. B., C. L. B., and A. M. R.), a Ball State University Department of Biology Sigma Zeta research award (to B. J. S.), National Institutes of Health Grant GM046904 (to M. H.), a Ball State University Faculty Advance research award (to E. M. R.), an Indiana Academy of Science senior research grant (to E. M. R.), and National Institutes of Health Grant GM111713 (to E. M. R.). The authors declare that they have no conflicts of interest with the contents of this article. The content is solely the responsibility of the authors and does not necessarily represent the official views of the National Institutes of Health.

This article contains Fig. S1.

[1] Present address: Center for Medical Education, Indiana University School of Medicine, Muncie, IN 47306.

[2] Both authors contributed equally to this work.

[3] Present address: Diabetes and Complications Therapeutics Area, Eli Lilly and Co., Indianapolis, IN 46225.

[4] Present address: Dept. of Pathology and Laboratory Medicine, University of Wisconsin-Madison, Madison, WI 53711.

[5] To whom correspondence should be addressed. Tel.: 765-285-8805; Fax: 765-285-8804; E-mail: emrubenstein@bsu.edu.

[6] The abbreviations used are: ER, endoplasmic reticulum; APC, anaphase-promoting complex; CAT tail, C-terminal addition of alanine and threonine; CPY, carboxypeptidase Y; DHFR, dihydrofolate reductase; Endo H, endoglycosidase H; ERAD, ER-associated degradation; ERpQC, ER preemptive quality control; ERSU, ER surveillance; GPD, glyceraldehyde-3-phosphate dehydrogenase; GPI, glycosylphosphatidylinositol; INM, inner nuclear membrane; INMAD, inner nuclear membrane-associated degradation; K12, tract of twelve lysine residues; PTM, post-translational modification; RESET, rapid ER stress-induced export; SHRED, stress-induced homeostatically regulated protein degradation; SUS–GFP, self-ubiquitylating substrate tagged with green fluorescent protein; TBS, Tris-buffered saline; TBS/T, TBS supplemented with Tween 20; UPR, unfolded protein response; UPRE, unfolded protein response element; G6PDH, glucose-6-phosphate dehydrogenase.

inner nuclear membrane (INM), which is physically continuous with the ER, where it promotes the destruction of nucleoplasmic and integral membrane proteins (14, 15). Two additional E3 complexes, the transmembrane Asi complex (Asi1, Asi2, and Asi3) and the anaphase-promoting complex (APC), mediate protein quality control at the INM (16–18).

In general, ERAD E3s target distinct proteins based on the location and nature of the proteins' degradation signals, or degrons. Proteins possessing cytosolic and nucleoplasmic degrons are ubiquitylated by Doa10 in ERAD-C (19–21). Proteins with degrons in the ER lumen or within membrane-spanning segments are generally ubiquitylated by Hrd1 in ERAD-L or ERAD-M, respectively (22–24). Hrd1 also recognizes proteins that aberrantly or persistently engage the translocon via ERAD-T (25). The E3 Rkr1 targets translationally stalled ER-targeted proteins in ERAD-RA (ribosome-associated) (8, 26, 27). Doa10, Asi, and APC promote turnover of nuclear envelope proteins in INM-associated degradation (INMAD) (15–18, 28). These functional distinctions are not absolute. For example, Doa10 promotes degradation of some proteins with intramembrane degrons (29, 30), and Ubr1 redundantly recognizes a subset of Doa10 and Hrd1 substrates (9, 30). An E3-independent degradation mechanism for relieving obstructed translocons was recently identified in which the zinc metalloprotease Ste24 cleaves engineered translocon-clogging proteins (31).

Following the discovery of the UPR, additional ER stress-sensing mechanisms have been identified that reduce the burden of aberrant proteins in the ER. The ER stress surveillance (ERSU) signaling pathway, mediated by the Slt2 mitogen-activated protein kinase, prevents inheritance of cortical ER containing aggregated proteins during ER stress (32, 33). ER stress also promotes lysosomal destruction of ER-resident proteins by at least two mechanisms: the rapid ER stress-induced export (RESET) pathway, in which misfolded glycosylphosphatidylinositol (GPI)-anchored proteins are trafficked to the lysosome via the secretory pathway (34), and the activation of autophagy of ER subdomains (micro-ER-phagy) (35). In macro-ER-phagy, segments of ER are also targeted for lysosomal destruction (36, 37); however, this mechanism has not been shown to be induced by ER stress. In the recently identified stress-induced homeostatically regulated protein degradation (SHRED) pathway, ER stress accelerates Ubr1-dependent degradation of misfolded cytosolic proteins and ER-localized proteins with misfolded cytosolic domains (38). In mammals, a subset of ER-targeted proteins exhibit translocational attenuation during ER stress, presumably as a preemptive measure to reduce the burden of unfolded proteins in the ER (39). This is likely mediated in part by the recently identified function of HRD1 in targeting secretory proteins prior to translocon insertion in a mechanism termed ER preemptive quality control (ERpQC) (40, 41).

Despite the expanding catalogue of characterized ER stress-response mechanisms, not all consequences of ER stress are known or understood. ER stress is a feature of several human diseases, including metabolic and neurodegenerative disorders, some forms of cancer, inflammation and immune syndromes, and mental illness (42–46). Prolonged ER stress leads to cell death, and at least one class of anticancer medications exerts its toxic effects on malignant cells by inducing ER stress (47, 48).

In this work, we systematically analyzed the effect of ER stress on degradation of a panel of ER and INM quality control substrates. We found that ER stress did not substantially alter the degradation profiles of model substrates for Doa10 or Rkr1. However, despite well-documented induction of Hrd1 machinery by the UPR (2), degradation of model luminal and translocon-associated substrates of Hrd1 exhibited strong sensitivity to ER stress. By contrast, degradation of Hrd1 substrates with intramembrane degrons proceeded with normal kinetics in the face of ER stress, indicating Hrd1 is not broadly inhibited during stress. Furthermore, two Asi substrates demonstrated different sensitivities to ER stress. Divergent responses of ERAD and INMAD pathways mediated by the same ubiquitin ligase suggest novel layers of regulation of protein degradation by ER stress. Finally, a translocon-clogging substrate of Ste24 accumulated in a form consistent with prolonged translocon engagement. Impaired degradation of proteins that persistently engage the translocon is expected to curtail ER import of other proteins, thereby mitigating the impact of ER stress.

Results

ER stress impairs degradation of a Hrd1 ERAD-T substrate

N-terminal fusion of the *Deg1* degron from MATα2 to Sec62 converts the protein to a Hrd1 ERAD-T substrate (25). Following co-translational insertion of two transmembrane segments of Sec62, a portion of the N-terminal tail aberrantly translocates into the translocon (Fig. 1*A*). A disulfide bond forms between a portion of the *Deg1*-Sec62 N-terminal tail and the interior of the translocon, contributing to persistent channel engagement (25, 49). After aberrant translocon engagement, *Deg1*-Sec62 becomes progressively modified by glycosylation, causing the protein to migrate as multiple species by SDS-PAGE (Fig. 1*B*) (25). *Deg1*-Sec62 is also acetylated on its N terminus and on two internal lysine residues (50). Neither acetylation nor glycosylation are required for *Deg1*-Sec62 degradation (25, 50). However, glycosylation serves as a visual indicator of aberrant translocon engagement. This aberrant translocon engagement triggers Hrd1-dependent degradation of *Deg1*-Sec62, although the mechanism by which Hrd1 recognizes the protein remains unclear (25).

To determine the impact of ER stress on ERAD-T, we analyzed the degradation of *Deg1*-Sec62 by pulse-chase in the presence and absence of the ER-specific stressor tunicamycin, which blocks *N*-linked glycosylation. In untreated cells, *Deg1*-Sec62 exhibited characteristic modification and degradation over time (Fig. 1*C*). Strikingly, treatment of yeast with 1 μg/ml tunicamycin for 30 min prior to radioactive labeling of nascent protein profoundly impaired *Deg1*-Sec62 degradation. Observable post-translational modification (PTM) of *Deg1*-Sec62 was also strongly impaired. Increasing tunicamycin concentration to 10 μg/ml completely abrogated observable *Deg1*-Sec62 PTM. The effects of tunicamycin were rapid. Degradation and PTM were strongly impaired when tunicamycin incubation was reduced to 10 min prior to radiolabeling, but not when tunicamycin was present only during pulse labeling (Fig. 1*D*). Similarly, treatment with the reducing agent dithiothreitol (DTT) at a concentration of 6 mM strongly impaired *Deg1*-

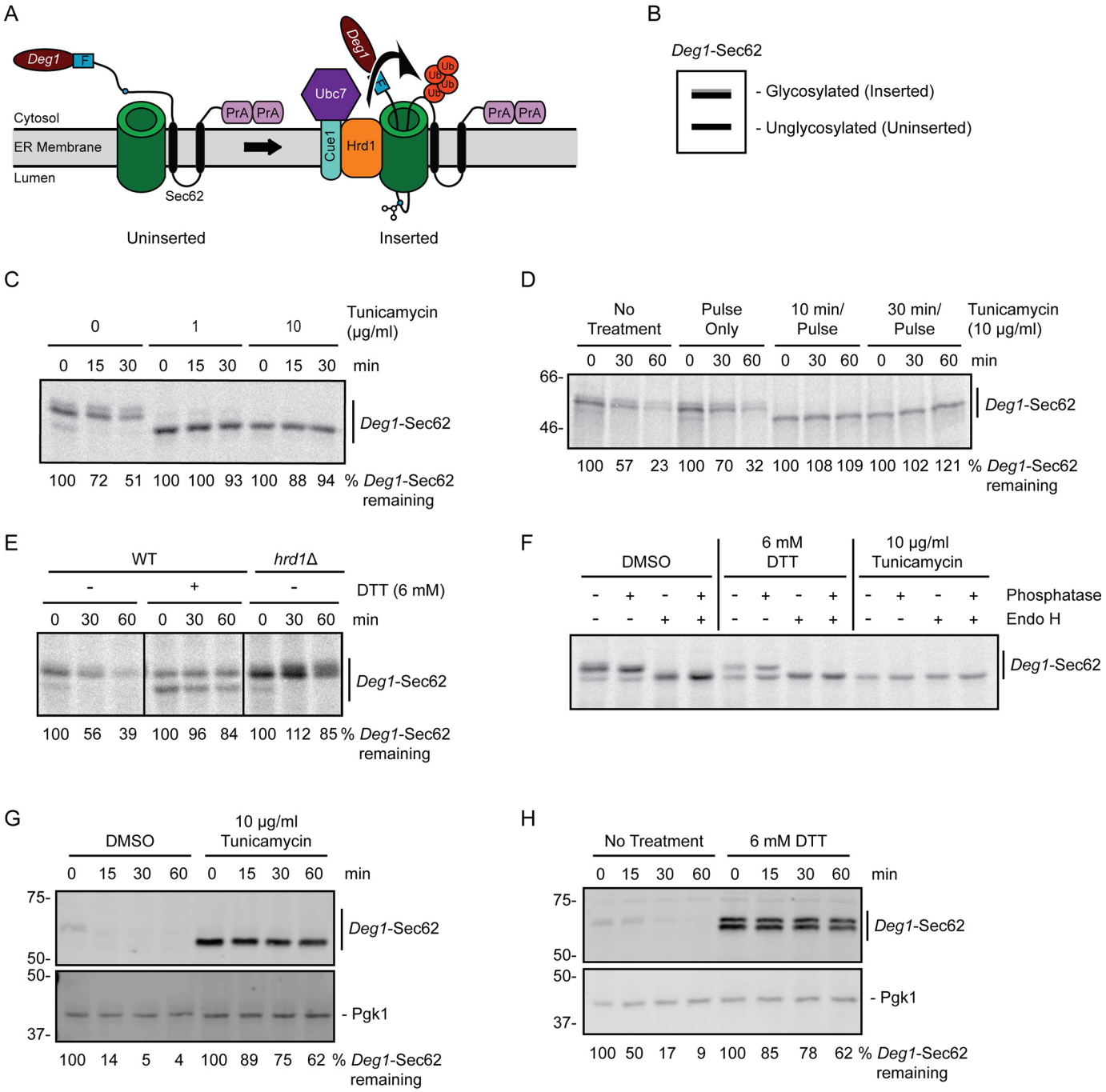

Figure 1. ER stress impairs degradation of a Hrd1 ERAD-T substrate. *A,* schematic depiction of *Deg1*-Sec62 prior to (uninserted) and following (inserted) aberrant translocon engagement. *Deg1*-Sec62 consists of *Deg1* (the N-terminal 67 amino acids from the yeast transcriptional repressor MATα2), a FLAG (*F*) epitope, the two-transmembrane protein Sec62, and two copies of the *S. aureus* protein A (*PrA*). Following translocon engagement, *Deg1*-Sec62 undergoes extensive PTM, including *N*-linked glycosylation, and is polyubiquitylated by Hrd1. The primary glycosylated asparagine residue is indicated as a *blue circle*. *Ub,* ubiquitin. *B,* virtual SDS-PAGE illustrates differential migration of *Deg1*-Sec62 based on glycosylation status. *C,* pulse-chase analysis of WT yeast expressing *Deg1*-Sec62 cultured in the presence of DMSO or tunicamycin at the indicated concentrations for 30 min. DMSO and tunicamycin were maintained at the same concentrations throughout pulse labeling. *D,* pulse-chase analysis of WT yeast expressing *Deg1*-Sec62 cultured in the presence of 10 μg/ml tunicamycin for the indicated times (or DMSO for 30 min). Tunicamycin and DMSO were maintained at the same concentrations throughout pulse labeling. *E,* pulse-chase analysis of WT or *hrd1*Δ yeast expressing *Deg1*-Sec62 cultured in the presence of 6 mM DTT (or no treatment) for 30 min. DTT was maintained at the same concentrations throughout pulse labeling. *F, doa10*Δ *hrd1*Δ yeast cells expressing *Deg1*-Sec62 were cultured in the presence 6 mM DTT, 10 μg/ml tunicamycin, or DMSO control for 30 min. DTT, tunicamycin, and DMSO were maintained at the indicated concentrations throughout pulse labeling. Immunoprecipitated *Deg1*-Sec62 was incubated in the presence or absence of Endo H and calf intestinal phosphatase as indicated. *G* and *H*, cycloheximide chase analysis of WT yeast expressing *Deg1*-Sec62 cultured in the presence of 10 μg/ml tunicamycin or DMSO (*G*) or 6 mM DTT or no treatment (*H*) for 1 h. Tunicamycin, DTT, or DMSO were maintained at the same concentration during incubation with cycloheximide. *Deg1*-Sec62 was detected with AlexaFluor-680–conjugated rabbit anti-mouse antibodies. Pgk1 served as a loading control. Where indicated, the percentage of *Deg1*-Sec62 remaining at each time point is presented *below the image*. For cycloheximide chase experiments, *Deg1*-Sec62 signal intensity was normalized to Pgk1. The experiment depicted in *C* was performed three times with tunicamycin at 0 and 10 μg/ml, and one time with tunicamycin at 1 μg/ml. Experiments depicted in *D* and *F* were performed one time. Experiments depicted in *E*, *G*, and *H* were performed three times.

Sec62 turnover (Fig. 1*E*); DTT causes ER stress by countering the normally oxidizing environment of the ER lumen. DTT also reduced PTM of *Deg1*-Sec62, but its impact on PTM was less pronounced than that of tunicamycin.

To characterize the PTM impaired by ER stressors, we incubated pulse-labeled *Deg1*-Sec62 with endoglycosidase H (Endo H) or calf intestinal phosphatase. The electrophoretic mobility of *Deg1*-Sec62 from unstressed cells exhibited strong sensitivity to Endo H, consistent with *N*-linked glycosylation (Fig. 1*F*). By contrast, *Deg1*-Sec62 exhibited little if any change in mobility after treatment with phosphatase, which is consistent with failure to detect *Deg1*-Sec62 phosphorylation in a recent biochemical analysis (50). Loss of Endo H-sensitive *Deg1*-Sec62 species following tunicamycin treatment confirmed that the compound completely inhibited *Deg1*-Sec62 *N*-glycosylation. DTT reduced the extent of or delayed glycosylation.

The pulse-chase experiments described above evaluated the degradation and modification of nascent *Deg1*-Sec62. Treatment for 1 h with either tunicamycin or DTT also strongly stabilized and impaired PTM of the steady-state *Deg1*-Sec62 population in cycloheximide-chase experiments (Fig. 1, *G* and *H*). Taken together, our results indicate that two different forms of ER stress strongly impair degradation and PTM of nascent and steady-state pools of a Hrd1 substrate that aberrantly engages the ER translocon.

ER stress differentially impacts degradation of Hrd1 substrates

Previous work indicated that degradation of the soluble Hrd1 ERAD-L substrate CPY* (a misfolded variant of carboxypeptidase Y possessing the G255R mutation) is inhibited by ER stress (2). Thus, one possible explanation for impairment of *Deg1*-Sec62 degradation is that Hrd1 catalytic activity is impaired by such stress. We analyzed the impact of ER stress on the degradation of a panel of Hrd1 substrates (depicted in Fig. 2*A*). Consistent with earlier reports, HA-tagged CPY* was strongly stabilized by both DTT and tunicamycin (Fig. 2*B*). Similar to *Deg1*-Sec62, both treatments impeded PTM of CPY*-HA, which is *N*-glycosylated. DTT and tunicamycin also stabilized the transmembrane ERAD-L substrate Erg3-13myc (51) to a similar extent as *HRD1* deletion (Fig. 2*C*).

We next evaluated the effect of ER stress on degradation of ERAD-M substrates 6myc-Hmg2 (3) and Pdr5*-HA (52). In contrast to ERAD-T and -L substrates, degradation of 6myc-Hmg2 (Fig. 2*D*) and Pdr5*-HA (Fig. 2*E*) was largely insensitive to DTT and tunicamycin; degradation of *Deg1*-Sec62 expressed in the same cells was markedly impaired during ER stress. These substrates were substantially stabilized by loss of Ubc7, the primary ubiquitin-conjugating enzyme that functions with Hrd1 (4). Finally, we evaluated the impact of ER stress on turnover of a self-ubiquitylating substrate (SUS-GFP) in which GFP and the Hrd1 RING domain are fused to a Myc-tagged transmembrane portion of Hmg1 (53, 54). Neither form of ER stress impaired turnover of SUS-GFP (Fig. S1). Thus, stabilization of model ERAD-T and ERAD-L substrates by ER stress is not due to broad impairment of Hrd1 ubiquitin ligase activity.

ER stress does not impair Doa10-dependent degradation

We evaluated the impact of ER stress on ERAD substrates targeted by Doa10. The nascent population of the transmembrane Doa10 ERAD-C substrate *Deg1*-Vma12 (Fig. 3*A*) (21) exhibited rapid degradation in the presence of ER stress in pulse-chase experiments (Fig. 3*B*). By contrast, this model Doa10 substrate was strongly stabilized by point mutations in the *Deg1* degron (*Deg1**, F18S and I22T (55)) that prevent Doa10-dependent degradation (21). Similarly, ER stress only mildly perturbed degradation of the steady-state population of *Deg1*-Vma12. This contrasted sharply with the strong stabilization of *Deg1*-Sec62 in the same cells (Fig. 3*C*).

Deg1-sec62† possesses a mutation in Sec62 (G127D of the fusion protein, equivalent to G37D of untagged Sec62) that substantially reduces aberrant translocation of its N-terminal tail (25, 56, 57). This variant is degraded predominantly by the Doa10 ERAD-C pathway. A minor subpopulation of this protein still undergoes aberrant translocation and retains Hrd1-dependent degradation (25). *Deg1*-sec62† was highly unstable, regardless of the presence of tunicamycin (Fig. 3*D*). Interestingly, a small fraction of *Deg1*-sec62† was stabilized by tunicamycin; this likely reflects the fraction of *Deg1*-sec62† that has become an ERAD-T (Hrd1) substrate by virtue of having undergone aberrant translocation.

ER stress does not impact Rkr1 substrate abundance

Vma12-K12-13myc is a model Rkr1 ERAD-RA substrate (Fig. 4*A*) (8). In this construct, N-terminally FLAG-tagged Vma12 is followed, in sequence, by two copies of protein A, 12 lysine residues (K12), and a 13myc epitope. The positively charged K12 sequence triggers ribosome stalling, likely via ionic attraction to the negatively charged ribosome exit tunnel (12, 58, 59). A virtual SDS-PAGE of lysates from WT and *rkr1*Δ cells expressing Vma12-K12-13myc is depicted in Fig. 4*B*. When Vma12-K12-13myc expressed in WT yeast cells is analyzed by SDS-PAGE and immunoblotting, two major populations are observed: a translationally stalled product (Vma12-K12) and the full-length translational read-through product (Vma12-K12-13myc). *RKR1* deletion increases abundance of the translationally-stalled protein relative to the full-length read-through product (8). Loss of *RKR1* also results in the appearance of multiple species migrating more slowly than Vma12-K12. We speculate these species represent Vma12-K12 molecules that have been modified by the C-terminal addition of alanine and threonine (CAT tails) as observed for soluble translationally-stalled substrates of Rkr1 (60, 61).

Incubation with ER stressors did not substantially alter Vma12-K12 mobility or abundance (Fig. 4*C*). We also have not observed an increase in the abundance of translationally stalled species of model soluble ER-targeted Rkr1 substrates in cells exposed to ER stress.[7] Our results suggest that ER stress does not inhibit Rkr1-dependent destruction of translationally stalled ERAD-RA substrates.

[7] B. W. Buchanan, L. N. Scanameo, and E. M. Rubenstein, unpublished observations.

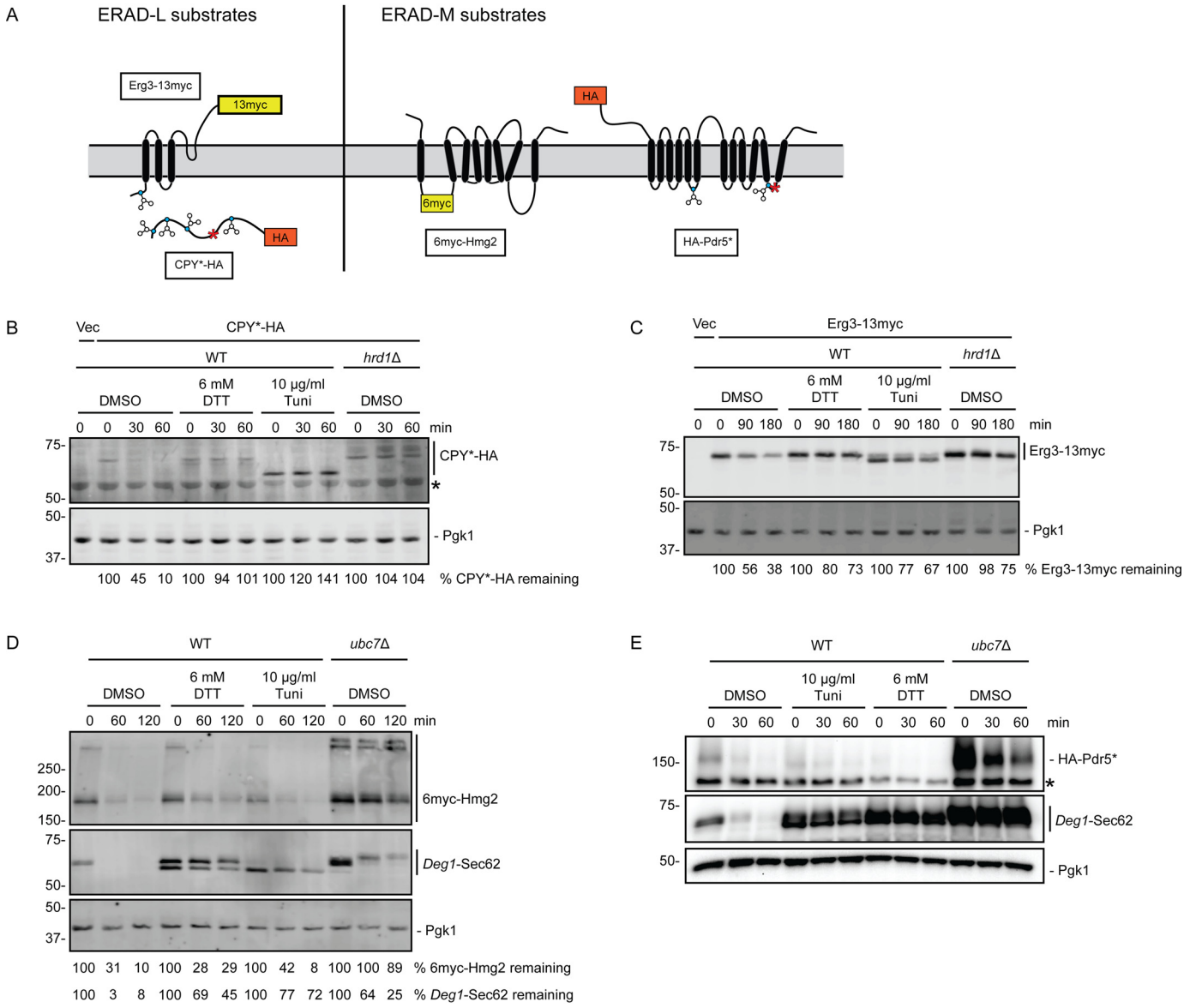

Figure 2. ER stress impairs degradation of Hrd1 ERAD-L substrates but not Hrd1 ERAD-M substrates. *A*, schematic of Hrd1 substrates investigated in this figure. *Blue circles* represent glycosylated amino acids. *Red asterisks* indicate destabilizing point mutations. *B–E*, cycloheximide chase analysis of yeast of the indicated genotypes harboring an empty vector (*Vec*) or expressing CPY*-HA (*B*), Erg3-13myc (*C*), 6myc-Hmg2 (*D*), or HA-Pdr5* (*E*) cultured in the presence of 6 mM DTT, 10 μg/ml tunicamycin, or DMSO for 1 h. DTT, tunicamycin, and DMSO were maintained at the same concentration during incubation with cycloheximide. *Asterisks* in *B* and *E* denote nonspecific bands. Cells analyzed in *D* and *E* also expressed *Deg1*-Sec62 as a control for ER stress induction. CPY*-HA and Pdr5*-HA were detected with anti-HA antibodies. Erg3-13myc and 6myc-Hmg2 were detected with anti-Myc antibodies. *Deg1*-Sec62 was detected with AlexaFluor-680 – conjugated rabbit anti-mouse antibodies (*D*) or peroxidase anti-peroxidase antibodies (*E*). Pgk1 served as a loading control. Where indicated, the percentage of substrate remaining (normalized to Pgk1) at each time point is presented *below the image*. We note that, relative to other experiments, *Deg1*-Sec62 exhibited weaker stabilization in the absence of *UBC7* in the cycloheximide chase presented in *D*; this may be related to differences in genetic background in the strains analyzed. Experiments depicted in *B–D* were performed three times. The experiment depicted in *E* was performed two times.

ER stress differentially impacts degradation of Asi substrates

We investigated the effect of ER stress on turnover of Erg11-FLAG and Vtc1-3HA, which are degraded via Asi-mediated INMAD upon mislocalization to the INM (Fig. 5*A*) (16, 17). Whereas ER stress perturbed Erg11-FLAG steady-state abundance, its turnover rate was largely unaffected relative to the impact of *ASI1* deletion (Fig. 5*B*). By contrast, ER stress stabilized Vtc1-3HA to a similar degree as loss of *ASI1* (Fig. 5*C*). Thus, Asi substrates are modestly, but differentially, sensitive to ER stress.

ER stress impairs degradation of a translocon-clogging substrate of Ste24

We analyzed the effects of ER stress on a second protein engineered to clog the ER translocon. This protein, dubbed "Clogger," consists of the soluble ER luminal Pdi1 protein followed, in sequence, by a rapidly folding variant of DHFR, three engineered glycosylation acceptor sequences, and an HA epitope (Fig. 6*A*) (31). The Pdi1 signal sequence promotes post-translational translocation. However, the rapidly folding DHFR causes a substantial fraction of the protein to clog the translo-

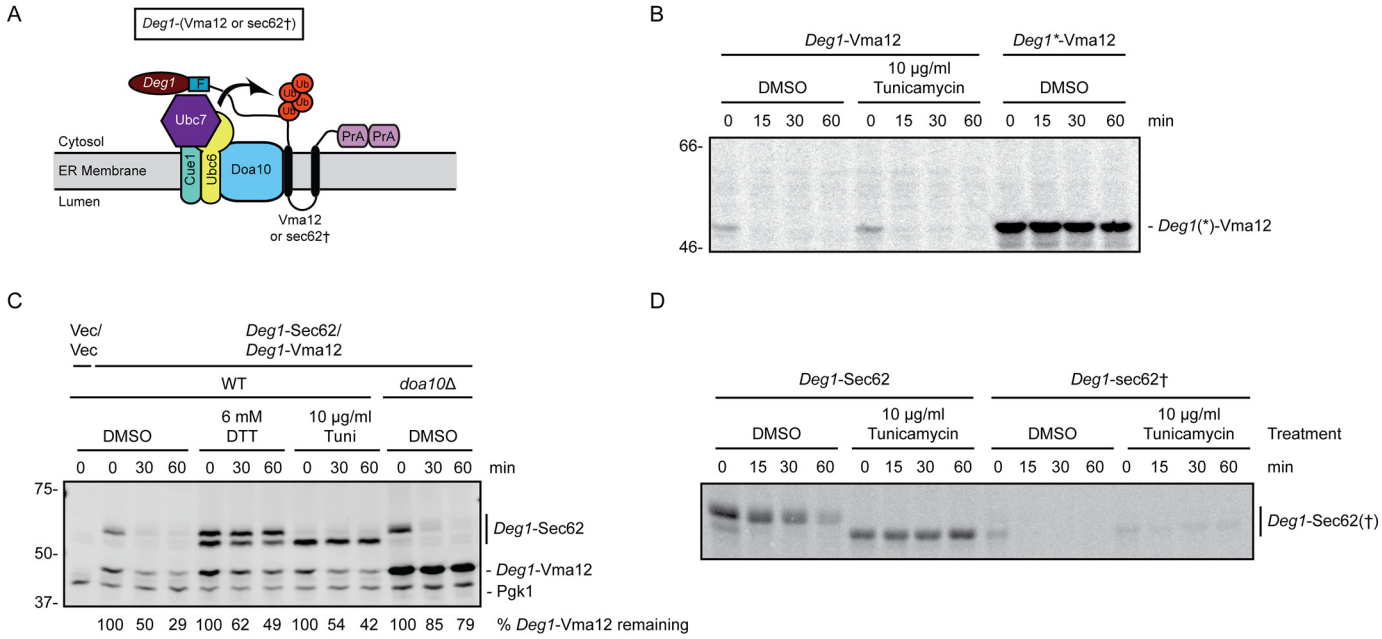

Figure 3. ER stress does not impair degradation of Doa10 ERAD-C substrates. *A,* schematic of Doa10 substrates investigated in this figure. *Deg1*-Vma12 consists of *Deg1*, a FLAG (*F*) epitope, the two-transmembrane protein Vma12, and two copies of the *S. aureus* protein A (*PrA*). *Deg1*-sec62† is *Deg1*-Sec62 with a point mutation that prevents aberrant translocon engagement, thus rendering the protein a Doa10 substrate. *Ub*, ubiquitin. *B* and *D,* pulse-chase analysis of WT yeast expressing *Deg1*(*)-Vma12 or *Deg1*-Sec62(†) cultured in the presence of 10 μg/ml tunicamycin or DMSO for 30 min. Tunicamycin and DMSO were maintained at the same concentration throughout pulse labeling. *C,* cycloheximide chase analysis of yeast of the indicated genotypes expressing *Deg1*-Vma12 and *Deg1*-Sec62 or harboring empty vectors (*Vec/Vec*), cultured in the presence of 6 mM DTT, 10 μg/ml tunicamycin, or DMSO for 1 h. DTT, tunicamycin, and DMSO were maintained at the same concentration during incubation with cycloheximide. *Deg1*-Sec62 and *Deg1*-Vma12 were detected with AlexaFluor-680–conjugated rabbit anti-mouse antibody. Pgk1 served as a loading control. The percentage of *Deg1*-Vma12 remaining at each time point (normalized to Pgk1) is indicated *below the image*. Experiments depicted in *B* and *D* were performed one time. The experiment depicted in *C* was performed three times.

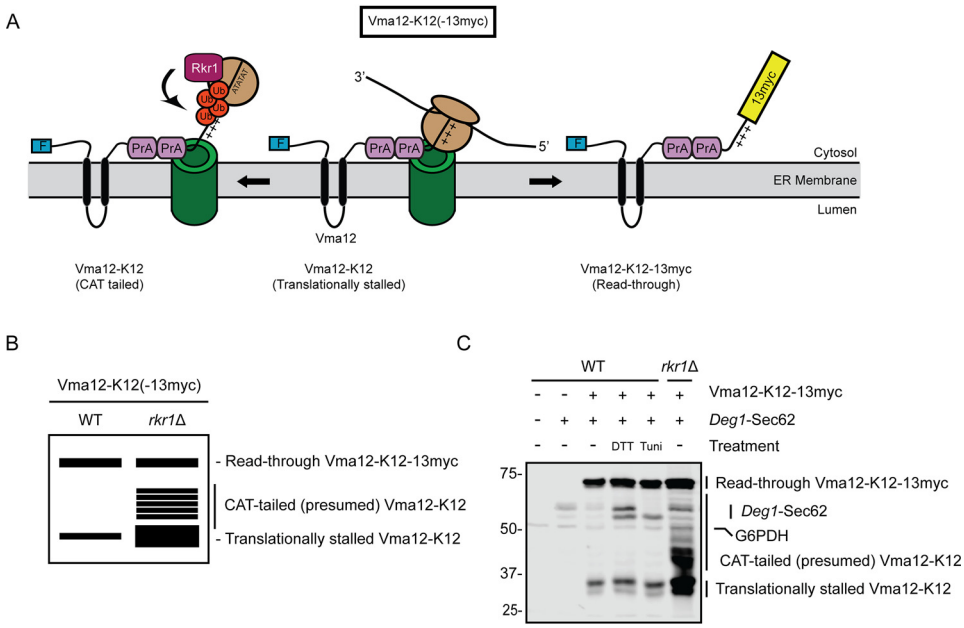

Figure 4. ER stress does not alter abundance of an Rkr1 ERAD-RA substrate. *A,* schematic of Vma12-K12-13myc, which consists of a FLAG epitope tag (*F*), the two-transmembrane protein Vma12, two copies of the *S. aureus* protein A (*PrA*), 12 lysine (*K12*) residues (depicted as sequential "+" symbols), and a 13myc epitope tag. After insertion of the two transmembrane segments of Vma12, K12 triggers translational stalling (*middle*). This is resolved by predicted C-terminal addition of alanine and threonine (AT) residues (CAT tailing), Rkr1-mediated ubiquitylation, and degradation (*left*) or release from stalling and translation of 13myc (*right*). *Ub,* ubiquitin. *B,* virtual SDS-PAGE illustrates differential migration of translationally stalled Vma12-K12, CAT-tailed Vma12-K12, and read-through product Vma12-K12-13myc in WT and *rkr1*Δ yeast lysates. *C,* yeast of the indicated genotypes harboring plasmids encoding Vma12-K12-13myc and *Deg1*-Sec62 (as a control for ER stress induction) or empty vectors were cultured in the presence of 6 mM DTT, 10 μg/ml tunicamycin, or DMSO (−) for 1 h prior to lysis and separation by SDS-PAGE. Vma12-K12-13myc was detected using anti-Myc antibodies, which bind to both 13myc and protein A. *Deg1*-Sec62 was detected with AlexaFluor-680–conjugated rabbit anti-mouse antibodies. G6PDH served as a loading control. Expression of Vma12-K12(-13myc) in *rkr1*Δ cells may increase *Deg1*-Sec62 levels, suggesting stabilized ERAD-RA substrates may cross-inhibit ERAD-T. The experiment depicted was performed four times.

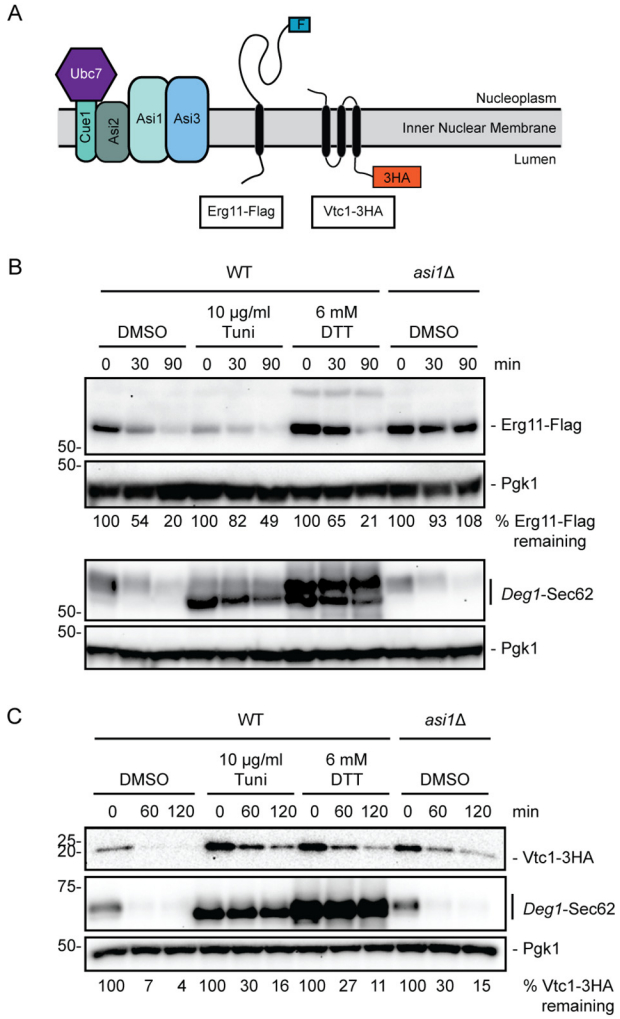

Figure 5. ER stress differentially affects degradation of Asi INMAD substrates. *A*, schematic of Asi substrates investigated in this figure. *B*, cycloheximide chase analysis of yeast of the indicated genotypes expressing Erg11-FLAG or *Deg1*-Sec62 cultured in the presence of 6 mM DTT, 10 μg/ml tunicamycin, or DMSO for 1 h. *C*, cycloheximide chase analysis of yeast of the indicated genotypes expressing Vtc1-3HA and *Deg1*-Sec62 cultured in the absence or presence of 6 mM DTT for 1 h. DTT, tunicamycin, and DMSO were maintained at the same concentration during incubation with cycloheximide. Erg11-FLAG was detected with anti-FLAG antibodies. Vtc1-3HA was detected with anti-HA antibodies. *Deg1*-Sec62 was detected with peroxidase anti-peroxidase antibodies. Pgk1 served as a loading control. The experiment depicted in *B* was performed two times. The experiment depicted in *C* was performed three times (with the exception of tunicamycin treatment, which was performed one time).

con. Because sequences upstream and downstream of the clogging moiety possess *N*-glycosylation acceptor sites, Clogger's ER insertion status can be assessed by comparing the relative abundance of differently migrating species (Fig. 6*B*). The fastest migrating species are nonglycosylated, cytosolic (uninserted) molecules. The slowest migrating species are fully glycosylated, completely translocated molecules. Species exhibiting intermediate migration are partially glycosylated, translocationally stalled molecules (31). The metalloprotease Ste24 cleaves the clogged form of this protein, thereby relieving translocon obstruction. Loss of Ste24 causes accumulation of faster migrating (*i.e.* clogged and cytosolic) forms of Clogger.

In the presence of DTT, faster migrating (presumably clogged and preinserted) Clogger species accumulated (Fig. 6*C*). Tunicamycin profoundly stabilized and impaired modification of Clogger. Thus, ER stress impairs degradation of Clogger and causes it to accumulate in a form consistent with persistent translocon engagement.

Deg1-Sec62 induces the UPR

ER stress impairs degradation of *Deg1*-Sec62 (Fig. 1) and Clogger (Fig. 6), two proteins that aberrantly engage the translocon. High-level expression of Clogger induces the UPR (31). To determine whether *Deg1*-Sec62 also induces the UPR, we transformed WT and *ubc7*Δ yeast with an empty vector or a plasmid encoding *Deg1*-Sec62 driven by the strong glyceraldehyde-3-phosphate dehydrogenase (GPD) promoter. These yeast expressed GFP under the control of the unfolded protein response element (UPRE). Fluorescence intensity, measured by flow cytometry, is therefore a readout of ER UPR induction. *Deg1*-Sec62 expression caused an ~2-fold induction of the UPR in *ubc7*Δ cells, consistent with exacerbation of ER stress by persistent translocon engagement (Fig. 7).

ERAD-T and its inhibition during ER stress are independent of characterized ER stress-responsive pathways

ERAD-T impairment during ER stress was surprising, given that the UPR increases expression of ubiquitin ligases (including Hrd1) and chaperone proteins involved in ER quality control (2). We tested the hypothesis that the UPR selectively inhibits ERAD-T during stress. In this case, restoration of ERAD-T during stress in cells lacking the UPR transducer Ire1 would be predicted. However, impairment of *Deg1**-Sec62 degradation by ER stress was not mitigated by loss of Ire1. Furthermore, ERAD-T proceeded largely unimpeded in *ire1*Δ cells (Fig. 8*A*). Failure to splice *HAC1* mRNA confirmed UPR deficiency in *ire1*Δ cells (Fig. 8*B*).

We investigated whether mediators of other ER stress-responsive pathways are required for *Deg1**-Sec62 degradation or stabilization by ER stress. Deletion of the gene encoding the Slt2 kinase, which prevents transmission of stressed ER to daughter cells via the ERSU mechanism (32), did not stabilize *Deg1**-Sec62 under nonstress conditions or prevent its stabilization by tunicamycin (Fig. 8*A*). In mammalian cells, where the RESET pathway was first characterized, the p24 family member Tmp21 mediates ER export of GPI-anchored proteins during ER stress (34). Loss of the Tmp21 homologue Emp24, which results in a p24-null phenotype in yeast (62), did not impair *Deg1**-Sec62 degradation or ER stress-dependent stabilization (Fig. 8*C*). Finally, mutation of the SHRED mediator Ubr1, which ubiquitylates misfolded proteins during cellular stress (38), did not detectably alter *Deg1**-Sec62 degradation kinetics in the presence or absence of ER stress (Fig. 8*D*).

We note that the variant of *Deg1*-Sec62 (*Deg1**-Sec62) employed in experiments presented in Fig. 8 (and in Fig. 11, *A* and *C*) possesses point mutations in *Deg1* (F18S and I22T). These alterations do not affect aberrant translocon engagement or Hrd1-dependent degradation (25). This construct has been used interchangeably with *Deg1*-Sec62 to investigate Hrd1-dependent ERAD-T (25, 50).

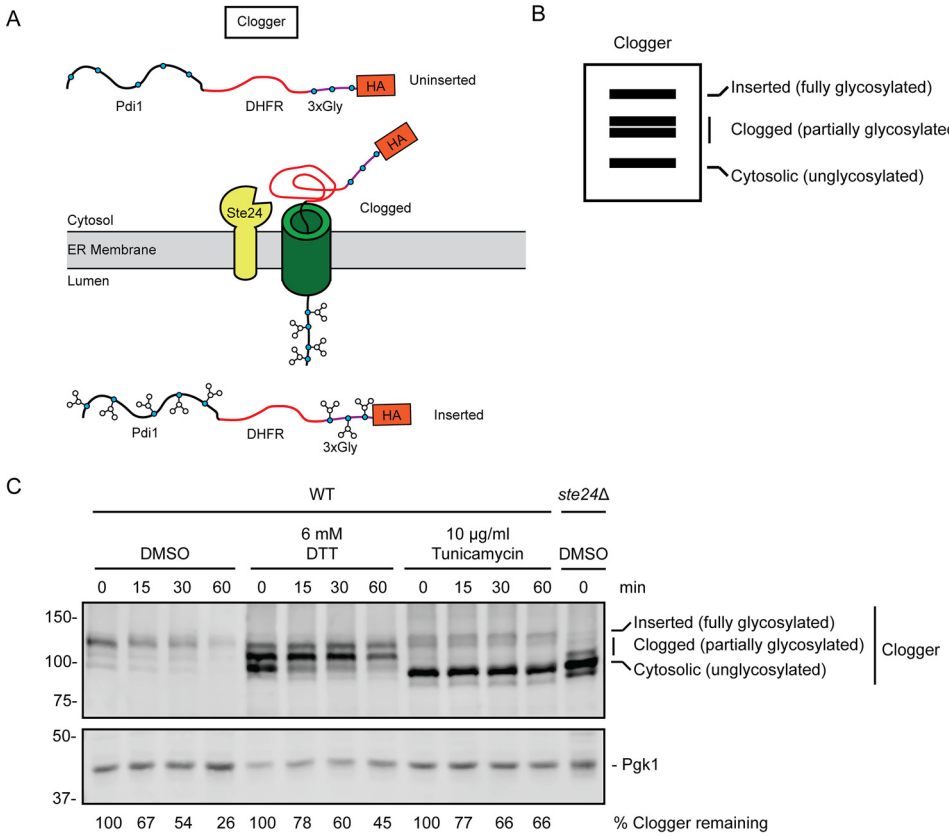

Figure 6. ER stress impairs degradation of a translocon-clogging substrate of Ste24. *A,* schematic of Clogger protein prior to (uninserted), during (clogged), and following (inserted) translocon engagement. Clogger consists of Pdi1 (which possesses glycosylation sites), DHFR, three additional glycosylation sites, and an HA epitope. Glycosylated amino acids are depicted as *blue circles*. *B,* virtual SDS-PAGE illustrates differential migration of uninserted, clogged, and inserted Clogger. *C,* cycloheximide chase analysis of yeast of the indicated genotypes expressing Clogger cultured in the presence of 6 mM DTT, 10 μg/ml tunicamycin, or DMSO for 1 h. DTT, tunicamycin, and DMSO were maintained at the same concentration during incubation with cycloheximide. Clogger was detected with anti-HA antibodies. Pgk1 served as a loading control. The percentage of Clogger remaining at each time point (normalized to Pgk1) is indicated *below the image*. The experiment depicted was performed three times.

Kar2 overexpression does not rescue Deg1-Sec62 degradation during ER stress

We tested whether overexpression of the multifunctional ER chaperone Kar2 suppresses inhibition of *Deg1*-Sec62 degradation during ER stress. We mildly overexpressed Kar2 by transforming WT yeast expressing *Deg1*-Sec62 with a centromeric plasmid encoding Kar2 (Fig. 9*A*). Western blot analysis confirmed a mild plasmid-dependent increase in Kar2 abundance. This mildly increased *KAR2* gene dosage did not accelerate *Deg1*-Sec62 degradation in the presence of DTT.

To more dramatically increase *KAR2* gene dosage, we transformed yeast expressing *Deg1*-Sec62 with a 2μ plasmid expressing *KAR2* from a yeast genomic library clone (63). Western blot analysis confirmed overexpression of Kar2 (Fig. 9*B*). In cells harboring the *KAR2* plasmid, we observed the appearance of a second, more slowly migrating species of Kar2, which likely corresponds to cytosolic Kar2 precursor that has retained its signal peptide prior to translocation (64). The accumulation of immature Kar2 in cells expressing Kar2 from a 2μ plasmid suggests an effective upper limit for ER-specific Kar2 overexpression. This moderately increased *KAR2* expression also did not accelerate *Deg1*-Sec62 degradation in the presence of DTT.

ER stress does not alter membrane association of Deg1-Sec62

ER stress limits *Deg1*-Sec62 PTM. Because these modifications largely occur in the ER lumen, we considered the possibility that ER stress alters translocation and membrane association of *Deg1*-Sec62, thereby impairing its ability to be recognized or degraded by Hrd1. We subjected ER-derived microsomes prepared from nonstressed and DTT-stressed cells to a variety of conditions to analyze the membrane association of *Deg1*-Sec62 (Fig. 10). *Deg1*-Sec62 was solubilized by detergent (Triton X-100). Consistent with membrane association, *Deg1*-Sec62 was not substantially solubilized following incubation with sodium chloride (which solubilizes cytosolic peripheral proteins) or sodium carbonate (which solubilizes both luminal and cytosolic peripheral proteins). Incubation of cells with DTT did not markedly alter the membrane association properties of *Deg1*-Sec62. Therefore, impairment of *Deg1*-Sec62 degradation by ER stress is not due to a stress-dependent change in *Deg1*-Sec62 membrane association.

ERAD-T is not broadly stress-sensitive

ER stress can also be induced by membrane aberrancy caused by inositol depletion (65). We cultured exponential-phase cells expressing *Deg1**-Sec62 in the presence or absence of inositol for 5 h. Inositol depletion induced the

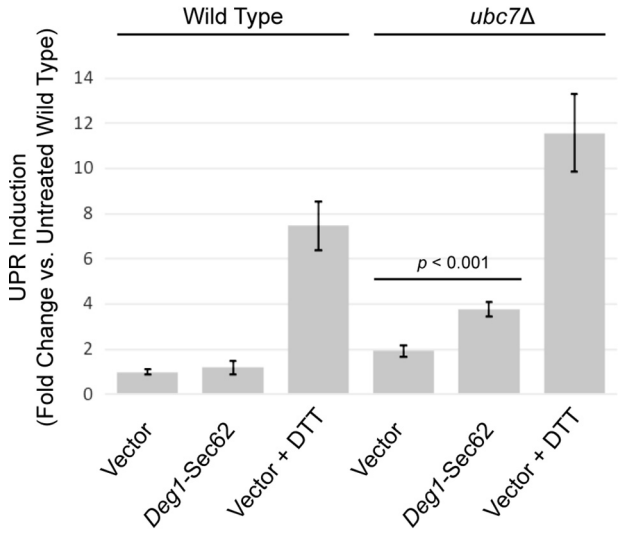

Figure 7. *Deg1*-Sec62 induces the unfolded protein response. Abundance of the UPR reporter GFP (driven by the UPRE) was analyzed by flow cytometry in WT and *ubc7*Δ yeast. Mid-exponential–phase cells harboring an empty vector or a plasmid encoding *Deg1*-Sec62 under the control of the GPD promoter were incubated in the absence (vector and *Deg1*-Sec62) or presence (*vector*) of 6 mM DTT for 1 h. The mean fluorescence intensity of 10,000 cells from each of nine cultures for each condition was normalized to the average mean fluorescence intensity of nine cultures of untreated WT cells harboring a vector. Mean fluorescence intensity ± standard error of the mean is presented. A two-tailed unpaired *t* test was performed to determine the significance of the difference between *ubc7*Δ cells harboring an empty vector and those expressing *Deg1*-Sec62.

UPR, as evidenced by increased UPRE-driven GFP expression (Fig. 11*A*). However, the rate of *Deg1**-Sec62 degradation was not impacted by inositol limitation.

DTT and tunicamycin induce ER stress by specifically promoting misfolding of ER-localized proteins. We asked whether heat shock, which causes protein misfolding throughout the cell, impairs *Deg1*-Sec62 destruction. We performed cycloheximide chase experiments to analyze *Deg1*-Sec62 degradation in cells cultured at 30 °C and shifted to 42 °C for 1 h and for the duration of the chase. Exposure to elevated temperatures did not stabilize *Deg1*-Sec62 in WT cells (Fig. 11*B*). Therefore, conditions associated with global protein misfolding are not sufficient to impair Hrd1-dependent destruction of an aberrant translocon-associated protein.

Finally, we determined whether oxidative stress affects *Deg1**-Sec62 turnover. The oxidant hydrogen peroxide induces the UPR in cultured myoblasts (66). Incubation of yeast in the presence of 0.4 mM hydrogen peroxide for 1 h did not affect *Deg1**-Sec62 degradation (Fig. 11*C*). Induction of oxidative stress-responsive GFP-tagged Rtc3 (67) in a parallel culture confirmed hydrogen peroxide activity (Fig. 11*D*).

Discussion

Our results reveal that ER stress differentially impacts ER and INM protein quality control proteolytic pathways. Model Doa10 ERAD-C and Rkr1 ERAD-RA substrates were largely unaffected by ER stress. Similarly, Hrd1-dependent degradation of proteins with intramembrane degrons proceeded with similar kinetics regardless of ER stress induction. However, destruction of three Hrd1 substrates (a soluble ERAD-L substrate, a transmembrane ERAD-L substrate, and an ERAD-T substrate) was specifically impaired by ER stress. Modification and turnover of a translocon-clogging substrate of Ste24 was also perturbed by ER stress. Finally, degradation of one of two tested Asi INMAD substrates was sensitive to ER stress.

During ER stress, translocation of a subset of proteins into the ER is slowed (39). Reduced ER chaperone availability correlates with and likely contributes to translocational attenuation, which is thought to be protective, reducing the load for the already burdened proteostasis machinery. Dampened translocon quality control during ER stress may be an additional adaptive mechanism in which undegraded channel-engaged proteins temporarily impede translocation of other polypeptides into the stressed ER.

Yeast and mammalian homologues of Hrd1 have been reported to physically interact with the translocon (41, 68). Interaction of mammalian HRD1 with the translocon was reported to increase ~1.5-fold during ER stress (41), an observation that would not be predicted by our results. Increased association of HRD1 with the translocon correlates with HRD1-dependent turnover of ER-targeted proteins prior to their translocation via ERpQC. By preemptively promoting degradation of secretory proteins prior to translocation, ERpQC may protect the stressed ER. We therefore speculate that regulation of Hrd1 by ER stress reduces protein load in the ER by two mechanisms: 1) stimulation of preemptive Hrd1-mediated targeting of secretory proteins prior to ER insertion, and 2) inhibition of Hrd1-dependent targeting of proteins that are already translocon-engaged.

Sensitivity of *Deg1*-Sec62 degradation to ER stress is consistent with an earlier observation that high-level expression of polyQ-expanded huntingtin protein both induces ER stress and impairs *Deg1*-Sec62 degradation (69). ERAD-T impairment is specific to particular subtypes of ER stress, as several different forms of stress expected to disrupt global proteostasis or ER homeostasis (elevated temperature, inositol limitation, and oxidative stress) did not impair *Deg1*-Sec62 degradation. Thus, misfolded proteins *per se* are likely not the direct signal impairing Hrd1-mediated destruction of translocon-associated proteins.

One potential trivial explanation for impairment of *Deg1*-Sec62 degradation is that ER stress prevents aberrant translocon engagement by *Deg1*-Sec62, which converts the protein into a Hrd1 substrate in the first place (25). We do not believe this is the cause for *Deg1*-Sec62 stabilization by ER stress for two reasons. First, *Deg1*-Sec62 becomes *N*-glycosylated in the presence of DTT (albeit in a delayed fashion), strongly suggesting that aberrant translocation of the fusion protein does occur. Second, mutations that prevent aberrant translocon engagement of *Deg1*-Sec62 cause a reversion of dependence of *Deg1*-Sec62 degradation from Hrd1 to Doa10 (25). Therefore, if ER stress blocks Hrd1-dependent degradation of *Deg1*-Sec62 by preventing translocon engagement, we would expect *Deg1*-Sec62 to become a Doa10 substrate and still be rapidly degraded; this is not observed. Consistently, we did not observe a difference in association of *Deg1*-Sec62 with ER membrane fractions in the presence or absence of ER stress.

Another possible explanation for impaired *Deg1*-Sec62 degradation is that ER stress prevents one or more PTMs

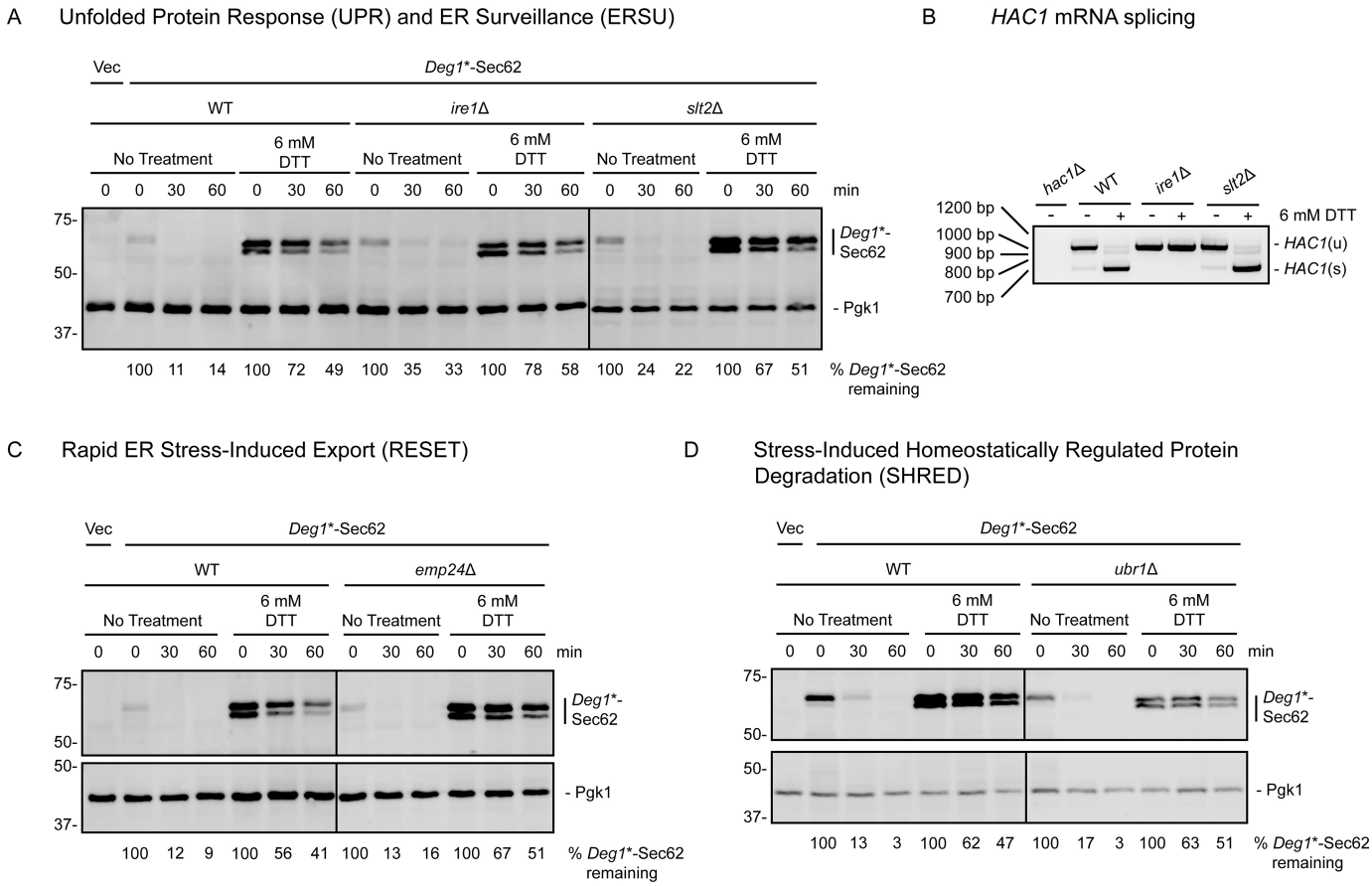

Figure 8. Characterized ER stress-sensing pathways do not regulate ERAD-T in the presence or absence of ER stress. *A, C,* and *D*, cycloheximide chase analysis of yeast of the indicated genotypes expressing *Deg1**-Sec62 or harboring an empty vector (*Vec*) cultured in the presence or absence of 6 mM DTT for 1 h. DTT was maintained at the same concentration during incubation with cycloheximide. *Deg1**-Sec62 was detected with peroxidase anti-peroxidase antibodies. Pgk1 served as a loading control. The percentage of *Deg1**-Sec62 remaining at each time point (normalized to Pgk1) is indicated *below the images*. *IRE1* (*A*), *SLT2* (*A*), *EMP24* (*C*), and *UBR1* (*D*) gene deletions were verified by PCR genotyping.[8] *B*, yeast of the indicated genotypes were incubated in the presence or absence of 6 mM DTT for 1 h prior to RNA extraction and RT-PCR to analyze *HAC1* mRNA splicing. Expected product sizes are 969 bp for unspliced *HAC1* (*HAC1*(*u*)) and 717 bp for spliced *HAC1* (*HAC1*(*s*)). Experiments depicted in *A*, *C*, and *D* were performed three times (with the exception of the *right panel of A*, which was performed two times). The experiment depicted in *B* was performed one time.

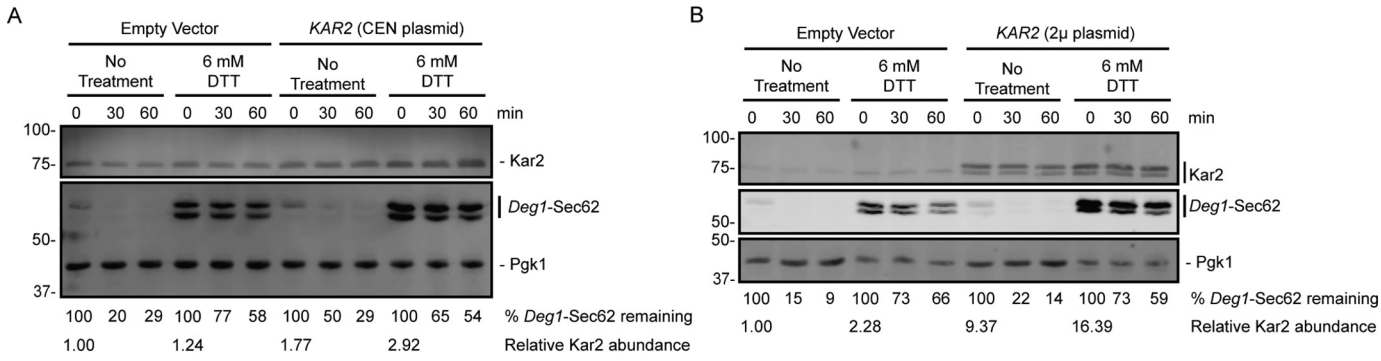

Figure 9. Kar2 overexpression does not rescue impaired ERAD-T during ER stress. Cycloheximide chase analysis of WT yeast expressing *Deg1*-Sec62 and harboring low-copy (centromeric) (*A*) or high-copy (2μ) (*B*) plasmids encoding Kar2 (or matching empty vector controls) cultured in the presence of 6 mM DTT or no treatment for 1 h. DTT was maintained at the same concentration during incubation with cycloheximide. *Deg1*-Sec62 was detected with AlexaFluor-680–conjugated rabbit anti-mouse antibodies. Kar2 was detected with anti-Kar2 antibodies. Pgk1 served as a loading control. The percentage of *Deg1*-Sec62 remaining at each time point (normalized to Pgk1) and Kar2 steady-state abundance relative to *Empty Vector/No Treatment* controls (normalized to Pgk1) are indicated *below the images*. Experiments depicted were performed three times.

required for recognition by Hrd1. However, neither glycosylation nor acetylation are required for *Deg1*-Sec62 degradation (25, 50). Although it remains possible that uncharacterized PTMs contribute to *Deg1*-Sec62 degradation, no available evidence suggests this is the case. The mechanism by which DTT delays modification of *Deg1*-Sec62 remains unclear. Redox perturbation may alter the structure or intermolecular interactions of enzymes required for glycosylation or

[8] C. L. Broshar and E. M. Rubenstein, unpublished observations.

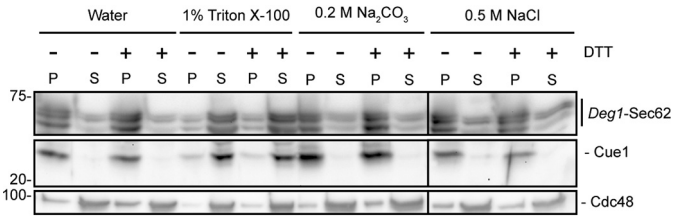

Figure 10. ER stress does not alter *Deg1*-Sec62 membrane association. ER-derived microsomes were prepared from *hrd1*Δ yeast expressing *Deg1*-Sec62 that had been cultured in the presence or absence of 6 mM DTT for 1 h. Microsomal fractions were incubated in the presence of water, 1% Triton X-100, 0.5 M sodium carbonate, or 0.5 M sodium chloride before being separated into pellet (*P*) and supernatant (*S*) fractions and solubilized. *Deg1*-Sec62 was detected with peroxidase anti-peroxidase antibodies. Cue1 and Cdc48 were detected by anti-Cue1 and anti-Cdc48 antibodies, respectively. The experiment depicted was performed two times (with the exception of sodium chloride treatment, which was performed one time).

substrate molecules in a manner that precludes efficient modification.

Unperturbed degradation of a subset of Hrd1 substrates argues against complete Hrd1 inhibition during ER stress. We speculate that one or more proteins sense ER stress and specifically inhibit Hrd1-dependent degradation of translocon-associated proteins. Our experiments argue against roles for the UPR, ERSU, RESET, and SHRED stress-sensing pathways in impeding the destruction of translocon-associated proteins during stress, unless they function redundantly.

It is possible that an as yet unidentified ERAD-T co-factor functions in a novel ER stress-sensing mechanism and becomes limiting for translocon-associated protein degradation. Stress-dependent changes in expression and complex association of Hrd1 cofactors have been observed (70). Another possibility is that one or more protein(s) sensitive to redox and glycosylation state mediate the effect of ER stress on degradation. Efforts to identify and characterize factors that regulate Hrd1-dependent degradation of translocon-engaged proteins are underway.

ER stress may similarly impair targeting of the translocon-associated clientele of Ste24. Accumulation of higher-mobility species suggests that the translocon-engaged form of Clogger is enriched in the presence of DTT. DTT-dependent changes in Clogger mobility were not observed in a previous investigation (31). This difference may be related to differences in treatment protocol between the two studies. In our experiments, cultures were incubated in the presence of 6 mM DTT for 1 h; in the experiments described in Ref. 31, yeast were incubated in the presence of 5 mM DTT for 4 h. It is possible that short- and long-term responses to ER stress differ.

Both Clogger and *Deg1*-Sec62 overexpression mildly induce the UPR (Fig. 7) (31). On its face, this runs counter to our suggestion that persistent translocon engagement protects against ER stress by reducing inward flux of nascent proteins. However, these two ideas can be reconciled with the following model. At basal levels of unfolded proteins in the ER, translocon clogging may increase stress by preventing inward movement of proteostasis machinery. By contrast, at higher levels of stress, nonspecifically stemming ER import may minimize the luminal burden of unfolded proteins.

Why does ER stress impair ERAD-L and not ERAD-M? Following Hrd1-mediated ubiquitylation, both ERAD-L and ERAD-M substrates must undergo protein extraction from the ER into the cytosol (retrotranslocation) prior to proteasome-mediated degradation (71). ERAD-L and ERAD-M substrates have different requirements for retrograde transport, and ER stress may only impair ERAD-L retrotranslocation (54, 71).

Finally, ER stress impacts Asi complex substrates in subtly different ways. Induction of ER stress alters the steady-state abundance of Erg11-FLAG without dramatically changing its rate of degradation. By contrast, ER stress impedes turnover of Vtc1-3HA to a similar degree as deletion of *ASI1*. These results imply that Asi substrates may be degraded and regulated via distinct modalities reminiscent of the multitude of Hrd1-mediated degradation mechanisms.

Unperturbed degradation of several proteins in the presence of tunicamycin and DTT appears to contradict a previous report of global proteasome inhibition by ER stress (72). However, although the earlier study reported acute stabilization of a subset of unstable proteins, degradation of a metabolically-labeled cytosolic protein was observed to proceed with similar kinetics in the absence and presence of stress. Mild accumulation of this protein during stress was observed over a longer time course following transient proteasome inhibition. These results argue for minor, indirect effects of ER stress on global protein degradation. In a more recent proteomics investigation, ER stress accelerated the proteasomal degradation of a subset of physiological proteins, while stabilizing others (73), consistent with divergent effects of ER stress on different protein populations.

Experimental procedures

Yeast and plasmid methods

Yeast were cultured at 30 °C in standard growth medium as described previously (49). Plasmids were introduced to yeast by the lithium acetate transformation procedure (74). Yeast strains and plasmids used in this study are presented in Tables 1 and 2, respectively. Yeast strains were generated by standard gene replacement methods and yeast mating, sporulation, and haploid selection (74, 75). Plasmids pVJ343, pVJ411, and pVJ463 were constructed by subcloning BamHI/HindIII fragments containing *Deg1*-Vma12, *Deg1**-Sec62, or *Deg1*-Sec62, respectively, from plasmids constructed in a previous study (25) into expression vectors with the desired promoter and auxotrophic marker gene (76, 77).

For galactose induction of Clogger, which is driven by the *GAL1/10* promoter, yeast were cultured overnight in selective medium containing 2% raffinose as the carbon source. Overnight cultures were diluted in fresh medium containing 4% galactose and cultured until cells reached mid-exponential growth.

For inositol limitation experiments, cells were cultured until they reached mid-exponential growth in medium containing inositol (prepared using yeast nitrogen base without amino acids). Cells were washed six times in medium lacking inositol (prepared using yeast nitrogen base without amino acids and inositol) and incubated in medium lacking inositol for 5 h.

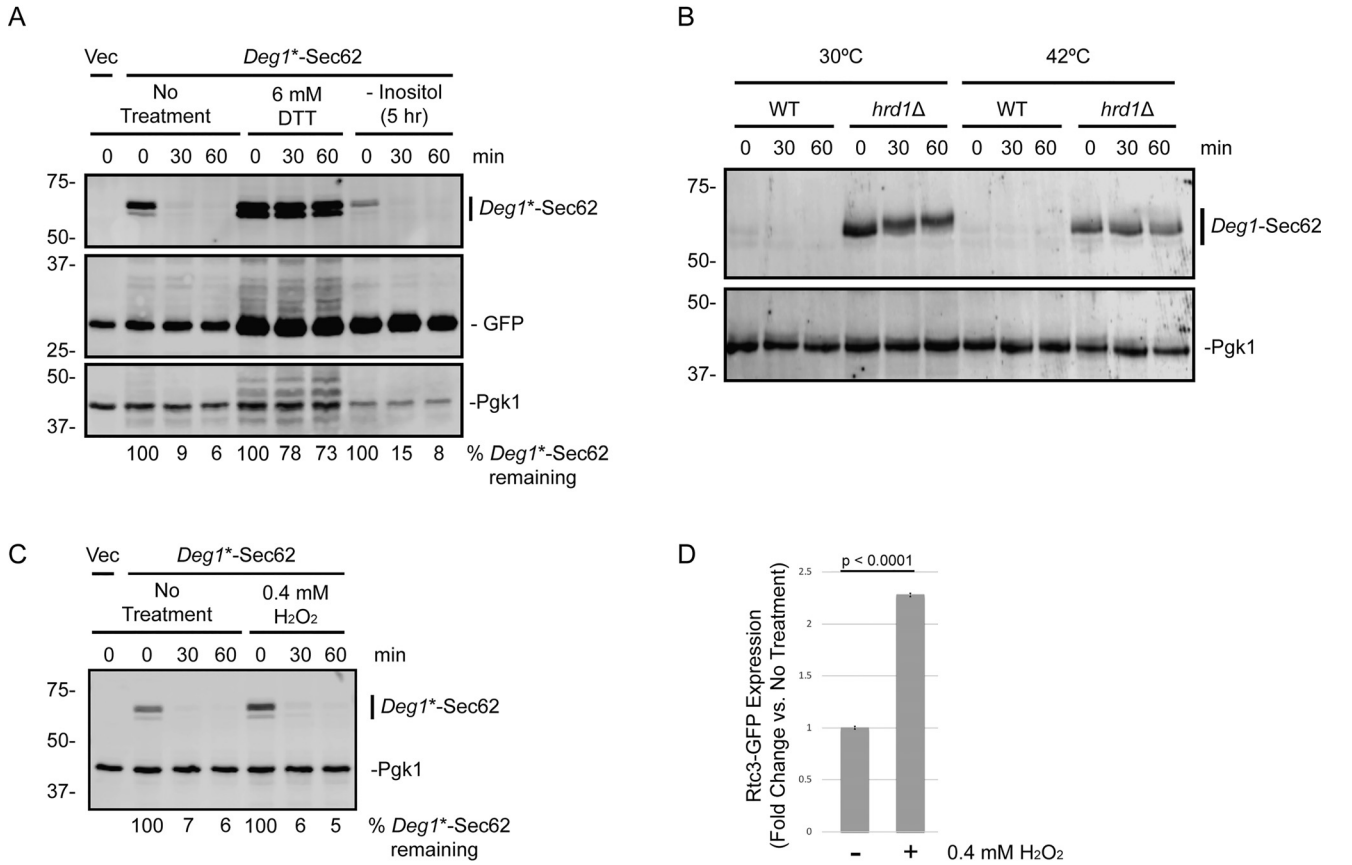

Figure 11. ERAD-T is not broadly stress-sensitive. *A,* cycloheximide chase analysis of WT yeast harboring an empty vector (*Vec*) or expressing *Deg1**-Sec62 cultured in inositol-rich medium in the presence or absence of 6 mM DTT for 1 h or shifted to inositol-free medium for 5 h. Cells also possessed a plasmid encoding GFP (driven by the UPRE). DTT concentration and inositol abundance were maintained during incubation with cycloheximide. *B,* cycloheximide chase analysis of WT yeast expressing *Deg1*-Sec62 cultured at 30 °C in the presence or absence of 6 mM DTT or shifted to 42 °C in the absence of 6 mM DTT for 1 h. Temperatures were maintained during incubation with cycloheximide. *C,* cycloheximide chase analysis of WT yeast harboring an empty vector or expressing *Deg1**-Sec62 in the presence or absence of 0.4 mM hydrogen peroxide (H_2O_2) for 1h. H_2O_2 concentrations were maintained during incubation with cycloheximide. *D,* in parallel to experiment depicted in *C*, mid-exponential phase yeast expressing oxidant-responsive Rtc3-GFP were analyzed by flow cytometry following incubation in the presence of 0.4 mM H_2O_2 for 1 h. The mean fluorescence intensity for each culture was normalized to the average mean fluorescence intensity of three repeats of untreated cells. Mean fluorescence intensity ± standard error of the mean is presented for three repeats of 10,000 cells for each condition. *A–C*, Pgk1 served as a loading control. *A* and *C*, percentage of *Deg1**-Sec62 remaining at each time point (normalized to Pgk1) is indicated *below the images*. Experiments depicted were performed three times.

Pulse-chase analysis

Pulse-chase analysis was performed as described previously (25, 78). Briefly, yeast cells were labeled with 20 μCi of Tran^{35}S-label (MP Biomedicals) per 1 OD_{600} unit of cells at 30 °C for 10 min in medium lacking methionine and cysteine. Chases were performed in the presence of excess unlabeled methionine and cysteine. *Deg1* fusion proteins were immunoprecipitated with anti-FLAG M2 affinity resin (Sigma) (Fig. 1, *D–F*) or sequential incubation with anti-*Deg1* antibody (79) and recombinant protein A– cross-linked agarose A (Repligen; Figs. 1*C* and 3, *B* and *D*). Immunoprecipitated proteins were separated by SDS-PAGE. Gels were analyzed by autoradiography, using a Storm 860 Phosphorimager system and ImageQuant 5.2 software (Molecular Dynamics). Figures for which molecular weight markers are not available (Figs. 1, *C*, *E* and *F*, and 3*D*) portray experiments performed on variants of proteins analyzed multiple times elsewhere in this study in experiments that include molecular weight markers.

Endoglycosidase H and calf intestinal phosphatase treatment

Cells were radiolabeled as described for pulse-chase experiments, and FLAG-tagged *Deg1*-Sec62 was immunoprecipitated with anti-FLAG M2 affinity resin. After five washes of resin with wash buffer (150 mM NaCl, 50 mM Hepes, pH 7.5, 5 mM EDTA, 1% Triton X-100, and 0.1% SDS), two additional equilibrating washes were performed with NEBuffer 4 (New England Biolabs). The resin was resuspended in 50 μl of NEBuffer 4 that had been supplemented with potassium acetate, pH 5.6, to a final concentration of 80 mM. 0.005 units of Endo H (Roche Applied Science), 10 units of calf intestinal phosphatase (New England Biolabs), both, or neither were added to the resin suspension. Samples were incubated at 37 °C for 3 h with gentle mixing approximately every 10 min. 1× Laemmli sample buffer was added, and samples were heated to 100 °C for 5 min.

Cell lysis

For experiments presented in Figs. 1, *G* and *H*, 2, *B–D*, 3*C*, 4*C*, 6*C*, 8, *A*, *C*, and *D*, 9, *A* and *B*, and 11, *A–C*, yeast were lysed as described previously (80, 81). Briefly, 2.5 OD_{600} units of yeast

Table 1
Yeast strains used in this study

Name	Alias	Genotype	Source	Figs.
VJY6	MHY500	*MATa his3-200 leu2-3,112 ura3-52 lys2-801 trp1-1 gal2*	78	1, *C*, *E*, *G*, and *H*, 2, *B*, *C*, and *E*, 3, *B*–*D*, 5*B*, 7, 9, *A* and *B*, and 11, *A* and *B*
VJY7	MHY1685	*MATa his3-200 leu2-3,112 ura3-52 lys2-801 trp1-1 gal2 doa10Δ::HIS3*	19	3*C*
VJY8	MHY1702	*MATa his3-200 leu2-3,112 ura3-52 lys2-801 trp1-1 gal2 doa10Δ::HIS3 hrd1Δ::LEU2*	19	1*F* and 10
VJY9	MHY2822	*MATa his3-200 leu2-3,112 ura3-52 lys2-801 trp1-1 gal2 hrd1Δ::LEU2*	19	1*E*
VJY10	MHY6198	*MATa his3-200 leu2-3,112 ura3-52 lys2-801 trp1-1 gal2 hrd1Δ::KanMX4*	This study	2, *B* and *C*
VJY29	MHY7719	*MATα ade2–101 met2 lys2-801 his3Δ200 trp1Δ leu2Δ ura3-52::6MYC-HMG2 hmg1Δ::LYS2 hmg2Δ::HIS3*	This study	2*D*
VJY33	MHY2972	*MATa his3Δ1 leu2Δ0 ura3Δ0*	88	1*D* and 4*C*
VJY35	MHY1661/ RHY665	*MATα ade2–101 met2 lys2-801 his3Δ200 trp1::hisG ura3-52::6MYC-HMG2 hmg1Δ::LYS2 hmg2Δ::HIS3 ubc7Δ::HIS3*	89	2*D*
VJY38	MHY7723	*MATa his3Δ1 leu2Δ0 ura3Δ0 met15Δ0 slt2Δ::kanMX4*	90	8, *A* and *B*
VJY50	MHY551	*MATa his3-200 leu2-3,112 ura3-52 lys2-801 trp1-1 gal2 ubc7Δ::LEU2*	78	2*E* and 7
VJY166	MHY5978	*MATa his3Δ1 leu2Δ0 ura3Δ0 met15Δ0 hac1Δ::kanMX4*	90	8*B*
VJY173	MHY2177	*MATa his3Δ1 leu2Δ0 ura3Δ0 met15Δ0 ire1Δ::kanMX4*	90	8, *A* and *B*
VJY306	SKY342	*MATa his3Δ1 leu2Δ0 met15Δ0 ura3Δ0 rkr1Δ::hphMX4*	8	4*C*
VJY404	2378/29	*MATa his3Δ1 leu2Δ0 met15Δ0 ura3Δ0 HO::NatR-Galp-PDIClogger*	31	6*C*
VJY405	2379/29	*MATa his3Δ1 leu2Δ0 met15Δ0 ura3Δ0 HO::NatR-Galp-PDIClogger ste24Δ::pcgURA*	31	6*C*
VJY476	BY4741	*MATa his3Δ1 leu2Δ0 met15Δ0 ura3Δ0*	90	8, *A*–8*C* and 11, *B* and *C*
VJY536	SSY122	*MATa leu2-3,112 trp1-1 ura3-1 his3-11,15*	38	8*D*
VJY540	SSY1782	*MATa leu2-3,112 trp1-1 ura3-1 his3-11,15 ubr1Δ::HIS3*	38	8*D*
VJY572	yMaM791	*MATa his3Δ1 leu2Δ0 met15Δ0 ura3Δ0 VTC1-3HA:hphNT1*	17	5*C*
VJY574	yMaM801	*MATa his3Δ1 leu2Δ0 met15Δ0 ura3Δ0 VTC1-3HA:hphNT1 asi1Δ::kanMX6*	17	5*C*
VJY616		*MATa his3Δ1 leu2Δ0 ura3Δ0 met15Δ0 RTC3-GFP:his5Sp*	91	11*D*
VJY620		*MATa his3Δ1 leu2Δ0 ura3Δ0 met15Δ0 emp24Δ::kanMX4*	90	8*C*
MHY8941		*MATa his3-200 leu2-3,112 ura3-52 lys2-801 trp1-1 gal2 asi1Δ::KanMX6*	Gift of C. Hickey	5*B*
MHY10483	ABM124	*MATα his3-200 leu2-3,112 ura3-52 lys2-801 trp1-1 gal2* P_{TDH3}*-SUS-GFP::TRP1*	This study	S1
MHY10487	ABM128	*MATα his3-200 leu2-3,112 ura3-52 lys2-801 trp1-1 gal2* P_{TDH3}*-SUS-GFP::TRP1 ubc7Δ::LEU2*	This study	S1

Table 2
Plasmids used in this study

Name	Alias	Yeast selection marker	Yeast plasmid type	Description	Source	Figs.
pHA-Pdr5*	pVJ1/pRH2312	*HIS3*	CEN	HA-tagged Pdr5*; Pdr5* = C1427Y	24	2*E*
YCp50-P_{PRC1}-CPY*-HA	pVJ2/pDN431	*URA3*	CEN	HA-tagged CPY* driven by native promoter; CPY* = G255R	92	2*B*
pRS313	pVJ26	*HIS3*	CEN	Empty vector	93	4*C* and 7
pRS316	pVJ27	*URA3*	CEN	Empty vector	93	2, *B* and *C*, 3*C*, 4*C*, 8, *A* and *C*, and 11*C*
p416-P_{MET25}-*Deg1*-FLAG-Sec62-2×ProtA	pVJ29	*URA3*	CEN	*Deg1*-Sec62 driven by *MET25* promoter	25	1, *D*, *E*, *G*, and *H*, 4*C*, 5, *B* and *C*, 10, and 11*B*, and S1
p414-P_{MET25}-*Deg1*-FLAG-Sec62-2×ProtA	pVJ30	*TRP1*	CEN	*Deg1*-Sec62 driven by *MET25* promoter	94	1, *C* and *F*, 2, *D* and *E*, 3, *C* and *D*, and 9, *A* and *B*
pRS314	pVJ39	*TRP1*	CEN	Empty vector	93	3*C*
pRS425	pVJ43	*LEU2*	2μ	Empty vector	95	9*B*
p415-P_{MET25}	pVJ122	*LEU2*	CEN	Empty vector with *MET25* promoter	76	8*D* and 11*A*
p414- P_{MET25}-*Deg1*-FLAG-Vma12-2×ProtA	pVJ172	*TRP1*	CEN	*Deg1*-Vma12 driven by *MET25* promoter	21	3*B*
p414-P_{MET25}-*Deg1**-FLAG-Vma12-2×ProtA	pVJ177	*TRP1*	CEN	*Deg1**-Vma12 driven by *MET25* promoter; *Deg1** = F18S, I22T	21	3*B*
p414-P_{MET25}-*Deg1*-FLAG-sec62†-2×ProtA	pVJ204	*TRP1*	CEN	*Deg1*-sec62† driven by *MET25* promoter; sec62† = sec62-1 = G127D	25	3*D*
p416-P_{MET25}-*Deg1**-Sec62-2×ProtA	pVJ317	*URA3*	CEN	*Deg1**-Sec62 driven by *MET25* promoter; *Deg1** = F18S, I22T	25	8, *A* and *C*, and 11*C*
p416-P_{GPD}-*Deg1*-FLAG-Vma12-2×ProtA	pVJ343	*TRP1*	CEN	*Deg1*-Vma12 driven by *TDH3* (*GPD*) promoter	This study	3*C*
p415-*P* P_{MET25}-*Deg1**-Sec62-2×ProtA	pVJ411	*LEU2*	CEN	*Deg1**-Sec62 driven by *MET25* promoter; *Deg1** = F18S, I22T	This study	8*D* and 11*A*
p413-P_{GPD}-FLAG-Vma12-ProtA-K12-13myc	pVJ457 (STK 07.4.3)	*HIS3*	CEN	Vma12-K12-13myc driven by *TDH3* (*GPD*) promoter	8	4*C*
p413-P_{GPD}-*Deg1*-Sec62-2×ProtA	pVJ463	*HIS3*	CEN	*Deg1*-Sec62 driven by *TDH3* (*GPD*) promoter	Gift of S. Kreft	7
pMRS366	pVJ512	*URA3*	CEN	Empty vector	96	9*A*
pMR397 (CEN)	pVJ513	*URA3*	CEN	Kar2 expression plasmid	96	9*A*
YGPM17a24	pVJ532	*LEU2*	2μ	Plasmid from Yeast Genomic Tiling Collection with genomic segment, including *KAR2* gene and promoter	63	9*B*
p416-P_{ERG3}-ERG3-13Myc	pVJ533/pLJ001	*URA3*	CEN	13myc-tagged Erg3 driven by native promoter	51	2*C*
pRS314-UPRE-GFP	pVJ552	*TRP1*	CEN	GFP driven by unfolded Protein Response Element (UPRE)	97	7 and 11*A*
pTDH3-SUS-GFP	pRH2900	*TRP1*	YIp	SUS-GFP driven by *TDH3* (*GPD*) promoter	54	Used to generate MHY10483
pRS316-Erg11-FLAG		*URA3*	CEN	FLAG-tagged Erg11 driven by native promoter	This study	5*B*

were harvested, suspended in 200 μl of 0.1 M NaOH, and incubated for 5 min at room temperature. Cells were pelleted, resuspended in 1× Laemmli sample buffer, and heated to 100 °C for 5 min. Lysates were subject to centrifugation to clear the preparations of insoluble material. The soluble fraction was separated by SDS-PAGE.

For experiments presented in Figs. 2*E*, and 5, *B* and *C*, and Fig. S1, yeast were lysed as described previously (82). Briefly, 2.5 OD_{600} units of yeast were harvested. NaOH was added to a final concentration of 0.26 M, and β-mercaptoethanol was added to a final concentration of 0.13 M. Cells were incubated on ice for 15 min. To precipitate proteins, TCA was added to a final concentration of 5%. Proteins were collected by centrifugation at 4 °C. Protein pellets were resuspended in 50 μl of TCA sample buffer (3.5% SDS, 0.5 M DTT, 80 mM Tris, 8 mM EDTA, 15% glycerol, and 0.1 mg/ml bromphenol blue) and incubated at 37 °C for 30 min. Insoluble material was pelleted by centrifugation prior to electrophoretic separation.

Cycloheximide-chase analysis

Cycloheximide-chase experiments were performed as described previously (83). Briefly, yeast were grown to mid-exponential phase at 30 °C, unless otherwise specified. Cells were concentrated to 2.5 OD_{600} units/ml in fresh media. Cycloheximide was added to a final concentration of 250 μg/ml. Aliquots of 2.4 OD_{600} units of cells (950 μl) were harvested at the indi-

cated times following cycloheximide addition, added to stop mix (final concentration 10 mM sodium azide, 0.25 mg/ml BSA), and placed on ice until the end of the chase, when all cells were lysed.

Microsome preparation and protein-membrane association analyses

Yeast microsomal membranes were prepared essentially as described previously (10, 25, 49). 10 OD_{600} units of cells were harvested, suspended in 1 ml of resuspension buffer (10 mM Tris, pH 9.4, and 10 mM DTT), and incubated at room temperature for 10 min. Cells were harvested by centrifugation, washed with spheroplast buffer (1 M sorbitol, 20 mM sodium phosphate, pH 7.5, 150 mM NaCl, and 2 mM DTT), and digested with 140 μg of zymolyase 100T (MP Biomedicals)/10 OD_{600} units of cells in spheroplast buffer for 20 min at 30 °C. Spheroplasts were harvested (5 min at 600 × *g* at 4 °C) and washed in spheroplast buffer containing 20 μg/ml pepstatin A, 1 mM EDTA, and 1× EDTA-free Complete Protease Inhibitor Mixture (Roche Applied Science). Spheroplasts were centrifuged again (5 min at 600 × *g* at 4 °C), resuspended in fractionation buffer (200 mM D-mannitol, 20 mM sodium phosphate, pH 7.5, and 150 mM NaCl) with protease inhibitors, and lysed by vortexing in the presence of glass beads for three 30-s pulses (1 min on ice between pulses). Unbroken cells and cellular debris were pelleted by centrifugation (5 min at 600 × *g* at 4 °C), and the supernatant was used as the microsomal preparation. Microsomes were incubated with sodium carbonate (final concentration 0.2 M, pH 11), Triton X-100 (final concentration 1% v/v), sodium chloride (final concentration 0.5 M), or no additive. Samples were maintained on ice for 15 min with occasional vortexing and then centrifuged (15 min at 13,000 × *g* at 4 °C). Supernatants were transferred to fresh tubes and preserved as the soluble fraction. To ensure samples had equal detergent concentrations, Triton X-100 was added to all supernatants that had not been initially solubilized with Triton X-100 (final concentration 1%); an equal volume of water was added to samples that had been previously solubilized by Triton X-100. Pellets were washed with fractionation buffer containing protease inhibitors and resuspended in fractionation buffer with 1% Triton X-100. 1× Laemmli sample buffer was added to all samples, prior to heating at 100 °C for 8 min and separation by SDS-PAGE.

Western blotting

Proteins were separated by SDS-PAGE and transferred to polyvinylidene difluoride membrane via wet transfer at 20 V for 1 h, 70 V for 2.5 h, or 30 V for 8 h at 4 °C. Membranes were blocked in a solution containing 5% skim milk in Tris-buffered saline (TBS: 50 mM Tris-base, 150 mM NaCl) at room temperature for 1 h or at 4 °C overnight. Membranes were probed in a solution containing 1% skim milk in TBS with 1% Tween 20 (TBS/T) and the appropriate antibody. The membranes were incubated in the presence of antibodies for 1 h at room temperature followed by three 5-min washes in TBS/T.

The following antibody dilutions were used: mouse anti-HA.11 (Clone 16B12; Covance and BioLegend) at 1:1,000–1:2,000; mouse anti-GFP (Clone JL-8; Clontech) at 1:1,000–1:2,000; mouse anti-phosphoglycerate kinase 1 (Pgk1; clone 22C5D8; Life Technologies, Inc.) at 1:5,000–1:40,000; mouse anti-FLAG (M2; Sigma) at 1:5,000; rabbit anti-glucose-6-phosphate dehydrogenase (G6PDH; Sigma) at 1:10,000; rabbit anti-KAR2 (clone y-115; Santa Cruz Biotechnology) at 1:2,000; rabbit anti-Cue1 (Hochstrasser laboratory) at 1:1,000; and rabbit anti-Cdc48 (gift of Thomas Sommer) at 1:1,000. Mouse primary antibodies were followed by incubation with either AlexaFluor-680–conjugated rabbit anti-mouse secondary antibody (Life Technologies, Inc.) at 1:20,000–1:40,000 or peroxidase-coupled sheep anti-mouse secondary antibody (GE Healthcare) at 1:5,000. Rabbit primary antibodies were followed by incubation with either peroxidase-coupled goat anti-rabbit (GE Healthcare) at 1:4,000 or IRDye-680RD–conjugated goat anti-rabbit secondary antibody (Li-Cor) at 1:40,000. AlexaFluor-680–conjugated rabbit anti-mouse antibody (Figs. 1, *G* and *H*, 2*D*, 3*C*, 4*C*, 8, *A, C,* and *D*, 9, *A* and *B*, and 11, *A–C*) or peroxidase anti-peroxidase (Sigma; 1:5,000; Figs. 2*E*, 5, *B* and *C*, and 10 and Fig. S1) were also used to directly detect the *Staphylococcus aureus* protein A epitope (found in variants of *Deg1*-Sec62, *Deg1*-Vma12, and Vma12-K12-13myc), which binds to mammalian Igs (84).

Membranes probed with fluorescently-labeled antibodies (Figs. 1, *G* and *H*, 2, *B–D*, 3*C*, 4*C*, 6*C*, 8, *A, C,* and *D*, 9, *A* and *B*, and 11, *A–C*) were imaged using an Odyssey CLx IR Imaging System and Image Studio Software (Li-Cor). Membranes probed with peroxidase-conjugated antibodies (Figs. 2*E*, 5, *B* and *C*, and 10, and Fig. S1) were visualized using enhanced chemiluminescence (GE Healthcare) and the G:BOX gel-imaging system and software (Syngene).

Flow cytometry

Flow cytometry was performed using cells expressing the indicated GFP-tagged proteins. Cells were cultured until they reached mid-exponential growth and were subjected to experimental treatments, as indicated. Mean GFP fluorescence of 10,000 cells in synthetic-defined medium was measured using the MACSquant Analyzer X.

Analysis of HAC1 mRNA splicing

HAC1 mRNA splicing was assessed using previously described methods with modifications (85–87). RNA was extracted from 1 OD_{600} unit of cells cultured to mid-exponential growth using RNeasy Mini (Qiagen) and DNA-free (Ambion) kits. cDNA was synthesized from 1 μg of total RNA using the iScript cDNA synthesis kit (Bio-Rad). The resulting cDNA was used as a template for PCRs as described (85). PCR products were analyzed on a 1.5% agarose gel and confirmed by DNA sequencing.

Author contributions—B. W. B., A. B. M., C. L. B., B. J. S., L. N. S., and E. M. R. formal analysis; B. W. B., C. L. B., A. M. R., B. J. S., M. H., and E. M. R. funding acquisition; B. W. B., A. B. M., C. L. B., A. M. R., B. J. S., L. N. S., and E. M. R. investigation; B. W. B., A. B. M., C. L. B., A. M. R., B. J. S., L. N. S., M. H., and E. M. R. writing-review and editing; M. H. and E. M. R. conceptualization; M. H. and E. M. R. supervision; E. M. R. project administration; E. M. R. writing-original draft.

Acknowledgments—We thank Andrew Kusmierczyk for insightful conversations at the genesis of this project. We thank Andrew Kusmierczyk, Douglas Bernstein, and members of the Hochstrasser, Kusmierczyk, Bernstein, and Rubenstein labs for helpful discussions throughout the project. We thank Christopher Hickey, Stefan Kreft, Randy Hampton, Christian Hirsch, Ernst Jarosch, Michael Knop, Matthias Meurer, Davis Ng, James Olzmann, Mark Rose, Randy Schekman, Sebastian Schuck, Maya Schuldiner, and Thomas Sommer for sharing plasmids, yeast strains, and antibodies. We thank Heather Bruns for assistance with flow cytometry. We thank Seth Horowitz for laboratory assistance during the project.

References

1. Wu, H., Ng, B. S., and Thibault, G. (2014) Endoplasmic reticulum stress response in yeast and humans. *Biosci. Rep.* **34,** e00118 CrossRef Medline
2. Travers, K. J., Patil, C. K., Wodicka, L., Lockhart, D. J., Weissman, J. S., and Walter, P. (2000) Functional and genomic analyses reveal an essential coordination between the unfolded protein response and ER-associated degradation. *Cell* **101,** 249–258 CrossRef Medline
3. Hampton, R. Y., Gardner, R. G., and Rine, J. (1996) Role of 26S proteasome and HRD genes in the degradation of 3-hydroxy-3-methylglutaryl–CoA reductase, an integral endoplasmic reticulum membrane protein. *Mol. Biol. Cell* **7,** 2029–2044 CrossRef Medline
4. Plemper, R. K., Bordallo, J., Deak, P. M., Taxis, C., Hitt, R., and Wolf, D. H. (1999) Genetic interactions of Hrd3p and Der3p/Hrd1p with Sec61p suggest a retro-translocation complex mediating protein transport for ER degradation. *J. Cell Sci.* **112,** 4123–4134 Medline
5. Wilhovsky, S., Gardner, R., and Hampton, R. (2000) HRD gene dependence of endoplasmic reticulum-associated degradation. *Mol. Biol. Cell* **11,** 1697–1708 CrossRef Medline
6. Bays, N. W., Gardner, R. G., Seelig, L. P., Joazeiro, C. A., and Hampton, R. Y. (2001) Hrd1p/Der3p is a membrane-anchored ubiquitin ligase required for ER-associated degradation. *Nat. Cell Biol.* **3,** 24–29 CrossRef Medline
7. Swanson, R., Locher, M., and Hochstrasser, M. (2001) A conserved ubiquitin ligase of the nuclear envelope/endoplasmic reticulum that functions in both ER-associated and Matα2 repressor degradation. *Genes Dev.* **15,** 2660–2674 CrossRef Medline
8. Crowder, J. J., Geigges, M., Gibson, R. T., Fults, E. S., Buchanan, B. W., Sachs, N., Schink, A., Kreft, S. G., and Rubenstein, E. M. (2015) Rkr1/Ltn1 ubiquitin ligase-mediated degradation of translationally stalled endoplasmic reticulum proteins. *J. Biol. Chem.* **290,** 18454–18466 CrossRef Medline
9. Stolz, A., Besser, S., Hottmann, H., and Wolf, D. H. (2013) Previously unknown role for the ubiquitin ligase Ubr1 in endoplasmic reticulum-associated protein degradation. *Proc. Natl. Acad. Sci. U.S.A.* **110,** 15271–15276 CrossRef Medline
10. Kreft, S. G., Wang, L., and Hochstrasser, M. (2006) Membrane topology of the yeast endoplasmic reticulum-localized ubiquitin ligase Doa10 and comparison with its human ortholog TEB4 (MARCH-VI). *J. Biol. Chem.* **281,** 4646–4653 CrossRef Medline
11. Deak, P. M., and Wolf, D. H. (2001) Membrane topology and function of Der3/Hrd1p as a ubiquitin-protein ligase (E3) involved in endoplasmic reticulum degradation. *J. Biol. Chem.* **276,** 10663–10669 CrossRef Medline
12. Bengtson, M. H., and Joazeiro, C. A. (2010) Role of a ribosome-associated E3 ubiquitin ligase in protein quality control. *Nature* **467,** 470–473 CrossRef Medline
13. Heck, J. W., Cheung, S. K., and Hampton, R. Y. (2010) Cytoplasmic protein quality control degradation mediated by parallel actions of the E3 ubiquitin ligases Ubr1 and San1. *Proc. Natl. Acad. Sci. U.S.A.* **107,** 1106–1111 CrossRef Medline
14. Deng, M., and Hochstrasser, M. (2006) Spatially regulated ubiquitin ligation by an ER/nuclear membrane ligase. *Nature* **443,** 827–831 CrossRef Medline
15. Boban, M., Pantazopoulou, M., Schick, A., Ljungdahl, P. O., and Foisner, R. (2014) A nuclear ubiquitin-proteasome pathway targets the inner nuclear membrane protein Asi2 for degradation. *J. Cell Sci.* **127,** 3603–3613 CrossRef Medline
16. Foresti, O., Rodriguez-Vaello, V., Funaya, C., and Carvalho, P. (2014) Quality control of inner nuclear membrane proteins by the Asi complex. *Science* **346,** 751–755 CrossRef Medline
17. Khmelinskii, A., Blaszczak, E., Pantazopoulou, M., Fischer, B., Omnus, D. J., Le Dez, G., Brossard, A., Gunnarsson, A., Barry, J. D., Meurer, M., Kirrmaier, D., Boone, C., Huber, W., Rabut, G., Ljungdahl, P. O., and Knop, M. (2014) Protein quality control at the inner nuclear membrane. *Nature* **516,** 410–413 CrossRef Medline
18. Koch, B. A., Jin, H., Tomko, R. J., Jr., and Yu, H. G. (2019) The anaphase-promoting complex regulates the degradation of the inner nuclear membrane protein Mps3. *J. Cell Biol.* **218,** 839–854 CrossRef Medline
19. Huyer, G., Piluek, W. F., Fansler, Z., Kreft, S. G., Hochstrasser, M., Brodsky, J. L., and Michaelis, S. (2004) Distinct machinery is required in *Saccharomyces cerevisiae* for the endoplasmic reticulum-associated degradation of a multispanning membrane protein and a soluble luminal protein. *J. Biol. Chem.* **279,** 38369–38378 CrossRef Medline
20. Metzger, M. B., Maurer, M. J., Dancy, B. M., and Michaelis, S. (2008) Degradation of a cytosolic protein requires endoplasmic reticulum-associated degradation machinery. *J. Biol. Chem.* **283,** 32302–32316 CrossRef Medline
21. Ravid, T., Kreft, S. G., and Hochstrasser, M. (2006) Membrane and soluble substrates of the Doa10 ubiquitin ligase are degraded by distinct pathways. *EMBO J.* **25,** 533–543 CrossRef Medline
22. Carvalho, P., Goder, V., and Rapoport, T. A. (2006) Distinct ubiquitin-ligase complexes define convergent pathways for the degradation of ER proteins. *Cell* **126,** 361–373 CrossRef Medline
23. Gauss, R., Sommer, T., and Jarosch, E. (2006) The Hrd1p ligase complex forms a linchpin between ER-lumenal substrate selection and Cdc48p recruitment. *EMBO J.* **25,** 1827–1835 CrossRef Medline
24. Sato, B. K., Schulz, D., Do, P. H., and Hampton, R. Y. (2009) Misfolded membrane proteins are specifically recognized by the transmembrane domain of the Hrd1p ubiquitin ligase. *Mol. Cell* **34,** 212–222 CrossRef Medline
25. Rubenstein, E. M., Kreft, S. G., Greenblatt, W., Swanson, R., and Hochstrasser, M. (2012) Aberrant substrate engagement of the ER translocon triggers degradation by the Hrd1 ubiquitin ligase. *J. Cell Biol.* **197,** 761–773 CrossRef Medline
26. Arakawa, S., Yunoki, K., Izawa, T., Tamura, Y., Nishikawa, S., and Endo, T. (2016) Quality control of nonstop membrane proteins at the ER membrane and in the cytosol. *Sci. Rep.* **6,** 30795 CrossRef Medline
27. von der Malsburg, K., Shao, S., and Hegde, R. S. (2015) The ribosome quality control pathway can access nascent polypeptides stalled at the Sec61 translocon. *Mol. Biol. Cell* **26,** 2168–2180 CrossRef Medline
28. Smoyer, C. J., and Jaspersen, S. L. (2019) Patrolling the nucleus: inner nuclear membrane-associated degradation. *Curr. Genet.* **65,** 1099–1106 CrossRef Medline
29. Habeck, G., Ebner, F. A., Shimada-Kreft, H., and Kreft, S. G. (2015) The yeast ERAD-C ubiquitin ligase Doa10 recognizes an intramembrane degron. *J. Cell Biol.* **209,** 261–273 CrossRef Medline
30. Ruggiano, A., Mora, G., Buxó, L., and Carvalho, P. (2016) Spatial control of lipid droplet proteins by the ERAD ubiquitin ligase Doa10. *EMBO J.* **35,** 1644–1655 CrossRef Medline
31. Ast, T., Michaelis, S., and Schuldiner, M. (2016) The protease Ste24 clears clogged translocons. *Cell* **164,** 103–114 CrossRef Medline
32. Babour, A., Bicknell, A. A., Tourtellotte, J., and Niwa, M. (2010) A surveillance pathway monitors the fitness of the endoplasmic reticulum to control its inheritance. *Cell* **142,** 256–269 CrossRef Medline
33. Piña, F. J., and Niwa, M. (2015) The ER Stress Surveillance (ERSU) pathway regulates daughter cell ER protein aggregate inheritance. *Elife 2015* **4,** CrossRef Medline
34. Satpute-Krishnan, P., Ajinkya, M., Bhat, S., Itakura, E., Hegde, R. S., and Lippincott-Schwartz, J. (2014) ER stress-induced clearance of misfolded GPI-anchored proteins via the secretory pathway. *Cell* **158,** 522–533 CrossRef Medline

35. Schuck, S., Gallagher, C. M., and Walter, P. (2014) ER-phagy mediates selective degradation of endoplasmic reticulum independently of the core autophagy machinery. *J. Cell Sci.* **127,** 4078–4088 CrossRef Medline
36. Lipatova, Z., and Segev, N. (2015) A role for Macro-ER-Phagy in ER quality control. *PLoS Genet.* **11,** e1005390 CrossRef Medline
37. Mochida, K., Oikawa, Y., Kimura, Y., Kirisako, H., Hirano, H., Ohsumi, Y., and Nakatogawa, H. (2015) Receptor-mediated selective autophagy degrades the endoplasmic reticulum and the nucleus. *Nature* **522,** 359–362 CrossRef Medline
38. Szoradi, T., Schaeff, K., Garcia-Rivera, E. M., Itzhak, D. N., Schmidt, R. M., Bircham, P. W., Leiss, K., Diaz-Miyar, J., Chen, V. K., Muzzey, D., Borner, G. H. H., and Schuck, S. (2018) SHRED is a regulatory cascade that reprograms Ubr1 substrate specificity for enhanced protein quality control during stress. *Mol. Cell* **70,** 1025–1037.e5 CrossRef Medline
39. Kang, S. W., Rane, N. S., Kim, S. J., Garrison, J. L., Taunton, J., and Hegde, R. S. (2006) Substrate-specific translocational attenuation during ER stress defines a pre-emptive quality control pathway. *Cell* **127,** 999–1013 CrossRef Medline
40. Kadowaki, H., Nagai, A., Maruyama, T., Takami, Y., Satrimafitrah, P., Kato, H., Honda, A., Hatta, T., Natsume, T., Sato, T., Kai, H., Ichijo, H., and Nishitoh, H. (2015) Pre-emptive quality control protects the ER from protein overload via the proximity of ERAD components and SRP. *Cell Rep.* **13,** 944–956 CrossRef Medline
41. Kadowaki, H., Satrimafitrah, P., Takami, Y., and Nishitoh, H. (2018) Molecular mechanism of ER stress-induced pre-emptive quality control involving association of the translocon, Derlin-1, and HRD1. *Sci. Rep.* **8,** 7317 CrossRef Medline
42. Corazzari, M., Gagliardi, M., Fimia, G. M., and Piacentini, M. (2017) Endoplasmic reticulum stress, unfolded protein response, and cancer cell fate. *Front. Oncol.* **7,** 78 CrossRef Medline
43. Grootjans, J., Kaser, A., Kaufman, R. J., and Blumberg, R. S. (2016) The unfolded protein response in immunity and inflammation. *Nat. Rev. Immunol.* **16,** 469–484 CrossRef Medline
44. Kim, Y., Santos, R., Gage, F. H., and Marchetto, M. C. (2017) Molecular mechanisms of bipolar disorder: progress made and future challenges. *Front. Cell. Neurosci.* **11,** 30 CrossRef Medline
45. Sozen, E., and Ozer, N. K. (2017) Impact of high cholesterol and endoplasmic reticulum stress on metabolic diseases: an updated minireview. *Redox Biol.* **12,** 456–461 CrossRef Medline
46. Xiang, C., Wang, Y., Zhang, H., and Han, F. (2017) The role of endoplasmic reticulum stress in neurodegenerative disease. *Apoptosis* **22,** 1–26 CrossRef Medline
47. Takenokuchi, M., Miyamoto, K., Saigo, K., and Taniguchi, T. (2015) Bortezomib causes ER stress-related death of acute promyelocytic leukemia cells through excessive accumulation of PML-RARA. *Anticancer Res.* **35,** 3307–3316 Medline
48. Utecht, K. N., and Kolesar, J. (2008) Bortezomib: a novel chemotherapeutic agent for hematologic malignancies. *Am. J. Health Syst. Pharm.* **65,** 1221–1231 CrossRef Medline
49. Scott, D. C., and Schekman, R. (2008) Role of Sec61p in the ER-associated degradation of short-lived transmembrane proteins. *J. Cell Biol.* **181,** 1095–1105 CrossRef Medline
50. Engle, S. M., Crowder, J. J., Watts, S. G., Indovina, C. J., Coffey, S. Z., and Rubenstein, E. M. (2017) Acetylation of N terminus and two internal amino acids is dispensable for degradation of a protein that aberrantly engages the endoplasmic reticulum translocon. *PeerJ* **5,** e3728 CrossRef Medline
51. Jaenicke, L. A., Brendebach, H., Selbach, M., and Hirsch, C. (2011) Yos9p assists in the degradation of certain nonglycosylated proteins from the endoplasmic reticulum. *Mol. Biol. Cell* **22,** 2937–2945 CrossRef Medline
52. Plemper, R. K., Egner, R., Kuchler, K., and Wolf, D. H. (1998) Endoplasmic reticulum degradation of a mutated ATP-binding cassette transporter Pdr5 proceeds in a concerted action of Sec61 and the proteasome. *J. Biol. Chem.* **273,** 32848–32856 CrossRef Medline
53. Garza, R. M., Sato, B. K., and Hampton, R. Y. (2009) *In vitro* analysis of Hrd1p-mediated retrotranslocation of its multispanning membrane substrate 3-hydroxy-3-methylglutaryl (HMG)-CoA reductase. *J. Biol. Chem.* **284,** 14710–14722 CrossRef Medline
54. Neal, S., Jaeger, P. A., Duttke, S. H., Benner, C., K Glass, C., Ideker, T., and Hampton, R. Y. (2018) The Dfm1 Derlin is required for ERAD retrotranslocation of integral membrane proteins. *Mol. Cell* **69,** 306–320.e4 CrossRef Medline
55. Johnson, P. R., Swanson, R., Rakhilina, L., and Hochstrasser, M. (1998) Degradation signal masking by heterodimerization of MATα2 and MATα1 blocks their mutual destruction by the ubiquitin-proteasome pathway. *Cell* **94,** 217–227 CrossRef Medline
56. Wittke, S., Dünnwald, M., and Johnsson, N. (2000) Sec62p, a component of the endoplasmic reticulum protein translocation machinery, contains multiple binding sites for the Sec-complex. *Mol. Biol. Cell* **11,** 3859–3871 CrossRef Medline
57. Deshaies, R. J., and Schekman, R. (1990) Structural and functional dissection of Sec62p, a membrane-bound component of the yeast endoplasmic reticulum protein import machinery. *Mol. Cell. Biol.* **10,** 6024–6035 CrossRef Medline
58. Dimitrova, L. N., Kuroha, K., Tatematsu, T., and Inada, T. (2009) Nascent peptide-dependent translation arrest leads to Not4p-mediated protein degradation by the proteasome. *J. Biol. Chem.* **284,** 10343–10352 CrossRef Medline
59. Lu, J., and Deutsch, C. (2008) Electrostatics in the ribosomal tunnel modulate chain elongation rates. *J. Mol. Biol.* **384,** 73–86 CrossRef Medline
60. Shen, P. S., Park, J., Qin, Y., Li, X., Parsawar, K., Larson, M. H., Cox, J., Cheng, Y., Lambowitz, A. M., Weissman, J. S., Brandman, O., and Frost, A. (2015) Protein synthesis. Rqc2p and 60S ribosomal subunits mediate mRNA-independent elongation of nascent chains. *Science* **347,** 75–78 CrossRef Medline
61. Kostova, K. K., Hickey, K. L., Osuna, B. A., Hussmann, J. A., Frost, A., Weinberg, D. E., and Weissman, J. S. (2017) CAT-tailing as a fail-safe mechanism for efficient degradation of stalled nascent polypeptides. *Science* **357,** 414–417 CrossRef Medline
62. Hirata, R., Nihei, C., and Nakano, A. (2013) Isoform-selective oligomer formation of *Saccharomyces cerevisiae* p24 family proteins. *J. Biol. Chem.* **288,** 37057–37070 CrossRef Medline
63. Jones, G. M., Stalker, J., Humphray, S., West, A., Cox, T., Rogers, J., Dunham, I., and Prelich, G. (2008) A systematic library for comprehensive overexpression screens in *Saccharomyces cerevisiae*. *Nat. Methods* **5,** 239–241 CrossRef Medline
64. Ng, D. T., Brown, J. D., and Walter, P. (1996) Signal sequences specify the targeting route to the endoplasmic reticulum membrane. *J. Cell Biol.* **134,** 269–278 CrossRef Medline
65. Promlek, T., Ishiwata-Kimata, Y., Shido, M., Sakuramoto, M., Kohno, K., and Kimata, Y. (2011) Membrane aberrancy and unfolded proteins activate the endoplasmic reticulum stress sensor Ire1 in different ways. *Mol. Biol. Cell* **22,** 3520–3532 CrossRef Medline
66. Pierre, N., Barbé, C., Gilson, H., Deldicque, L., Raymackers, J. M., and Francaux, M. (2014) Activation of ER stress by hydrogen peroxide in C2C12 myotubes. *Biochem. Biophys. Res. Commun.* **450,** 459–463 CrossRef Medline
67. Tsang, C. K., Liu, Y., Thomas, J., Zhang, Y., and Zheng, X. F. (2014) Superoxide dismutase 1 acts as a nuclear transcription factor to regulate oxidative stress resistance. *Nat. Commun.* **5,** 3446 CrossRef Medline
68. Schäfer, A., and Wolf, D. H. (2009) Sec61p is part of the endoplasmic reticulum-associated degradation machinery. *EMBO J.* **28,** 2874–2884 CrossRef Medline
69. Duennwald, M. L., and Lindquist, S. (2008) Impaired ERAD and ER stress are early and specific events in polyglutamine toxicity. *Genes Dev.* **22,** 3308–3319 CrossRef Medline
70. Nakatsukasa, K., Brodsky, J. L., and Kamura, T. (2013) A stalled retrotranslocation complex reveals physical linkage between substrate recognition and proteasomal degradation during ER-associated degradation. *Mol. Biol. Cell* **24,** 1765–1775, S1–S8 CrossRef Medline
71. Mehrtash, A. B., and Hochstrasser, M. (2019) Ubiquitin-dependent protein degradation at the endoplasmic reticulum and nuclear envelope. *Semin. Cell Dev. Biol.* **93,** 111–124 CrossRef Medline
72. Menéndez-Benito, V., Verhoef, L. G., Masucci, M. G., and Dantuma, N. P. (2005) Endoplasmic reticulum stress compromises the ubiquitin-proteasome system. *Hum. Mol. Genet.* **14,** 2787–2799 CrossRef Medline

73. Fabre, B., Livneh, I., Ziv, T., and Ciechanover, A. (2019) Identification of proteins regulated by the proteasome following induction of endoplasmic reticulum stress. *Biochem. Biophys. Res. Commun.* **517,** 188–192 CrossRef Medline
74. Guthrie, C., and Fink, G. R. (eds) (2004) *Guide to Yeast Genetics and Molecular and Cell Biology,* pp. 1–933, Elsevier, San Diego, CA
75. Goldstein, A. L., and McCusker, J. H. (1999) Three new dominant drug resistance cassettes for gene disruption in *Saccharomyces cerevisiae*. *Yeast* **15,** 1541–1553 CrossRef Medline
76. Mumberg, D., Müller, R., and Funk, M. (1994) Regulatable promoters of *Saccharomyces cerevisiae*: comparison of transcriptional activity and their use for heterologous expression. *Nucleic Acids Res.* **22,** 5767–5768 CrossRef Medline
77. Mumberg, D., Müller, R., and Funk, M. (1995) Yeast vectors for the controlled expression of heterologous proteins in different genetic backgrounds. *Gene* **156,** 119–122 CrossRef Medline
78. Chen, P., Johnson, P., Sommer, T., Jentsch, S., and Hochstrasser, M. (1993) Multiple ubiquitin-conjugating enzymes participate in the *in vivo* degradation of the yeast MATα2 repressor. *Cell* **74,** 357–369 CrossRef Medline
79. Hochstrasser, M., and Varshavsky, A. (1990) *In vivo* degradation of a transcriptional regulator: the yeast α2 repressor. *Cell* **61,** 697–708 CrossRef Medline
80. Kushnirov, V. V. (2000) Rapid and reliable protein extraction from yeast. *Yeast* **16,** 857–860 CrossRef Medline
81. Watts, S. G., Crowder, J. J., Coffey, S. Z., and Rubenstein, E. M. (2015) Growth-based determination and biochemical confirmation of genetic requirements for protein degradation in *Saccharomyces cerevisiae*. *J. Vis. Exp. 2015,* e52428 CrossRef Medline
82. Loayza, D., and Michaelis, S. (1998) Role for the ubiquitin-proteasome system in the vacuolar degradation of Ste6p, the a-factor transporter in *Saccharomyces cerevisiae*. *Mol. Cell. Biol.* **18,** 779–789 CrossRef Medline
83. Buchanan, B. W., Lloyd, M. E., Engle, S. M., and Rubenstein, E. M. (2016) Cycloheximide chase analysis of protein degradation in *Saccharomyces cerevisiae*. *J. Vis. Exp. 2016*, e53975 CrossRef Medline
84. Hjelm, H., Hjelm, K., and Sjöquist, J. (1972) Protein A from *Staphylococcus aureus*. Its isolation by affinity chromatography and its use as an immunosorbent for isolation of immunoglobulins. *FEBS Lett.* **28,** 73–76 CrossRef Medline
85. Miyazaki, T., Nakayama, H., Nagayoshi, Y., Kakeya, H., and Kohno, S. (2013) Dissection of Ire1 functions reveals stress response mechanisms uniquely evolved in *Candida glabrata*. *PLoS Pathog.* **9,** e1003160 CrossRef Medline
86. Scrimale, T., Didone, L., de Mesy Bentley, K. L., and Krysan, D. J. (2009) The unfolded protein response is induced by the cell wall integrity mitogen-activated protein kinase signaling cascade and is required for cell wall integrity in *Saccharomyces cerevisiae*. *Mol. Biol. Cell* **20,** 164–175 CrossRef Medline
87. Ryu, H. Y., Wilson, N. R., Mehta, S., Hwang, S. S., and Hochstrasser, M. (2016) Loss of the SUMO protease Ulp2 triggers a specific multichromosome aneuploidy. *Genes Dev.* **30,** 1881–1894 CrossRef Medline
88. Lewis, A., Felberbaum, R., and Hochstrasser, M. (2007) A nuclear envelope protein linking nuclear pore basket assembly, SUMO protease regulation, and mRNA surveillance. *J. Cell Biol.* **178,** 813–827 CrossRef Medline
89. Hampton, R. Y., and Bhakta, H. (1997) Ubiquitin-mediated regulation of 3-hydroxy-3-methylglutaryl–CoA reductase. *Proc. Natl. Acad. Sci. U.S.A.* **94,** 12944–12948 CrossRef Medline
90. Tong, A. H., Evangelista, M., Parsons, A. B., Xu, H., Bader, G. D., Pagé, N., Robinson, M., Raghibizadeh, S., Hogue, C. W., Bussey, H., Andrews, B., Tyers, M., and Boone, C. (2001) Systematic genetic analysis with ordered arrays of yeast deletion mutants. *Science* **294,** 2364–2368 CrossRef Medline
91. Huh, W. K., Falvo, J. V., Gerke, L. C., Carroll, A. S., Howson, R. W., Weissman, J. S., and O'Shea, E. K. (2003) Global analysis of protein localization in budding yeast. *Nature* **425,** 686–691 CrossRef Medline
92. Ng, D. T., Spear, E. D., and Walter, P. (2000) The unfolded protein response regulates multiple aspects of secretory and membrane protein biogenesis and endoplasmic reticulum quality control. *J. Cell Biol.* **150,** 77–88 CrossRef Medline
93. Sikorski, R. S., and Hieter, P. (1989) A system of shuttle vectors and yeast host strains designed for efficient manipulation of DNA in *Saccharomyces cerevisiae*. *Genetics* **122,** 19–27 Medline
94. Mayer, T. U., Braun, T., and Jentsch, S. (1998) Role of the proteasome in membrane extraction of a short-lived ER-transmembrane protein. *EMBO J.* **17,** 3251–3257 CrossRef Medline
95. Christianson, T. W., Sikorski, R. S., Dante, M., Shero, J. H., and Hieter, P. (1992) Multifunctional yeast high-copy-number shuttle vectors. *Gene* **110,** 119–122 CrossRef Medline
96. Rose, M. D., Misra, L. M., and Vogel, J. P. (1989) KAR2, a karyogamy gene, is the yeast homologue of the mammalian BiP/GRP78 gene. *Cell* **57,** 1211–1221 CrossRef Medline
97. Olzmann, J. A., and Kopito, R. R. (2011) Lipid droplet formation is dispensable for endoplasmic reticulum-associated degradation. *J. Biol. Chem.* **286,** 27872–27874 CrossRef Medline